SUPRAMOLECULAR HYDROGELS FOR REAGENT AND CATALYST DELIVERY

Charles Francis Edward Biddlecombe

Masters by Research
University of York
Chemistry

January 2022

Declaration of Authorship

I declare that this thesis is a presentation of original work, and I am its sole author. Where significant help has been given, this has been stated within the text. This work has not previously been presented for award at this, or any other, University. All sources are referenced within the bibliography.

Abstract

Hydrogels have found increasing use in widespread modern-day applications, including in the field of catalysis. Low-molecular weight gelators can be mixed and spatially shaped with polymer gelators to form a hybrid hydrogel bead. Beads of DBS-CONHNH$_2$/sodium alginate had an average diameter of 3 mm, and the beads made up of DBS-CONHNH$_2$/agarose had a larger distribution in diameter between 2-5 mm.

Hybrid hydrogel beads have been used for the support and growth of silver and palladium nanoparticles, which were used for the catalysis of nitro-aromatic reduction and Suzuki-Miyaura cross-couplings respectively. Both reactions were able to operate at room temperature in aqueous conditions. The hydrogel support was used for a silver nanoparticle catalysed 4-nitrophenol reduction, which achieved 43% yield, and a palladium nanoparticle catalysed 4-iodophenyl cross-coupling with phenyl boronic acid, which achieved 52% yield. The silver nanoparticle loaded alginate-based beads could be recycled to reduce 4-nitrophenol for a second time, although mechanical degradation of the beads prevented further recycles.

The two nanoparticle species were further added onto the same hydrogel support, giving a multi-nanoparticle loaded bead. The beads loaded with both silver and palladium nanoparticles were used for the Suzuki-Miyaura cross-coupling and 4-nitrophenol reduction, achieving a 52% and 43% yield respectively.

Palladium nanoparticle uptake was measured by UV-Vis and studied using Transmission Electron Microscopy (TEM), while silver nanoparticle uptake was measured using titration with sodium chloride and potassium chromate. Both nanoparticle species were also closely studied by TEM, where the silver nanoparticles were found to be 20-50 nm in diameter, while the palladium nanoparticles were between 1-10 nm.

The hybrid hydrogel bead is a versatile, simple-use catalyst tool for catalysis, that additionally provides a green approach to the field by improving recyclability for multiple reactions and negating the need for potentially dangerous and expensive ligands.

Contents

1. Introduction 8
    - 1.1. Hydrogel Structure and Formation 8
    - 1.2. Supramolecular Hydrogels 9
    - 1.3. Hydrogels in Transition Metal Catalysis 10
    - 1.4. DBS-CONHNH$_2$ 12
    - 1.5. Hybrid Hydrogels 15
    - 1.6. Aims and Objectives 16
2. Results and Discussion 17
    - 2.1. Gel Beads 17
    - 2.2. Silver Nanoparticles 20
    - 2.3. Palladium Nanoparticles 29
    - 2.4. Multi-Nanoparticle 38
3. Conclusion 42
4. Future Work 43
5. Experimental 44
6. Appendix 56
7. Bibliography 60

1. Introduction

1.1. Hydrogel Structure and Formation

Hydrogels are a well-known type of gel formed in water, that have found increasingly widespread use in modern day applications, including medicine, environmental remediation and other materials. Hydrogels are a three-dimensional material of cross-linked fibres that form a network to trap water or an aqueous solution, which forms a significant proportion of its weight.

In polymer hydrogels, common structural features of polymers that can form hydrogels include hydrophilic groups along the chain that provide strong interactions with the solvent, which help the gel absorb the water, after which dissolution into the sol phase is prevented by the cross-linking process.

The polymer gelates by cross-linking the many fibres together to trap the water molecules. Cross-linking can occur via either chemical methods, involving the formation of covalent bonds (Figure 1.1), or physical linking, where links between fibres involve intermolecular forces (Figure 1.2), such as ionic interactions or hydrogen bonding.[1] The junctions, the location where two polymer chains link in a gel, in a chemically cross-linked gel are fixed to a single position, while physically cross-linked gels have transient junctions that can move along the chain. This leads to physically cross-linked gels having a more dynamic and responsive nature than chemically cross-linked gels.

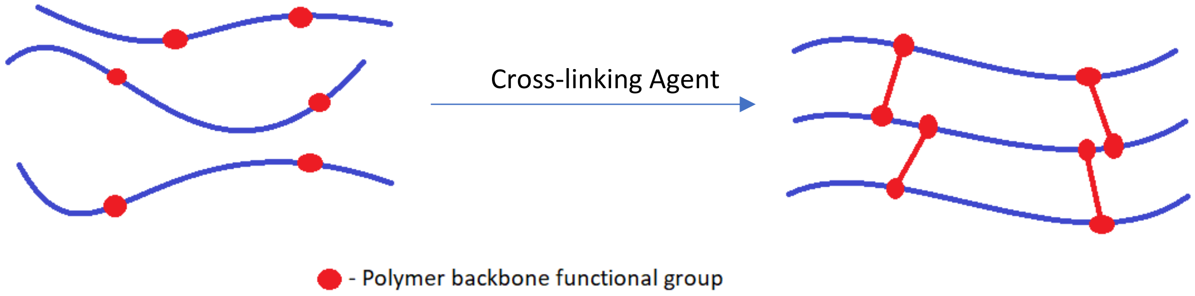

Figure 1.1: Schematic illustration of a chemically cross-linked gel via addition of chemical additive

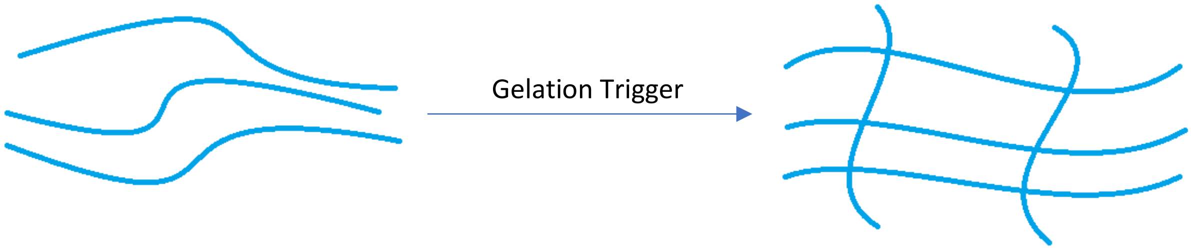

Figure 1.2: Schematic illustration of a physically cross-linked gel via hydrogen bonding and entanglement

The process to initiate cross-linking is activated by several gelation triggers. For example, gels that physically cross-link via hydrogen bonding typically need to be dissolved in the solvent by heating, where hydrogen bonds can be formed in the liquid-phase between chains, coiling them together and resulting in an extensively cross-linked network. For gels that form via ionic interactions, such as in sodium alginate, gelation can occur via the addition of a salt containing the complementary ion to the chains.[2]

Chemically cross-linked hydrogels require the addition of cross-linking agents to functionalise the polymer chain to form covalent bonds with other chains. One of the earliest examples of chemically cross-linked gels was poly(2-hydroxyethyl methacrylate) (pHEMA), which cross-linked via radical polymerisation with triethyleneglycol dimethacrylate (TEGDMA) as the additive.[3] Cross-linking can also occur with the addition of aldehydes,[4] enzymes[5] or high energy irradiation.[6] These agents however are often hazardous chemicals that can be toxic to environmental life, typically producing dangerous side-products and unwanted residues.

1.2. Supramolecular Hydrogels

Supramolecular hydrogels are a particular class of hydrogels that are not formed from long chain polymers, but from low-molecular-weight gelators (LMWGs).[7] LMWG's do not form chains via covalent bonding but using strong intermolecular forces between individual monomers to assemble, such as hydrogen bonding, π-π stacking and van der Waal's forces. Because of this, all LMWG's are inherently physically cross-linked gels with transient junctions, as no covalent bonds are made during cross-linking. As these interactions are non-covalent, the sol-gel phase transition is reversible.

Supramolecular hydrogels are assembled via intermolecular forces between the monomers, and these interactions can form when the monomers are dissolved in solution (for LMWG hydrogels) which allows for the initial stacking and formation of single fibrils. The interactions between these fibrils aggregates them into larger fibres which then entangle to form an extended cross-linked network because of hierarchical non-covalent interactions. The bulk solvent (water), although retaining its mobility on the molecular scale, is trapped within the entangled fibrous network by capillary forces, swelling the gel and giving the large majority of its weight.

Many LMWG's are derived from amino acids and peptides,[8] which see common use as supramolecular hydrogelators due to their high biocompatibility[9] and natural sourcing, with the peptide bond between amino acids giving strong hydrogen bonding. Some early work on peptide hydrogelators was done by Vegners *et al.* on a Fmoc-Leu-Asp which was used for the incorporation of the antiviral drug adamantanamine.[10] More recently, Abul-Haija and co-workers developed a multicomponent tripeptide hydrogel built from GHK (glycine-histidine-lysine) and FFD (diphenylalanine-aspartic acid) that ionically gelates in 30 mM $CuCl_{2\,(aq)}$.[11] Sugars have also been used as a biocompatible LMWG framework, such as the family of gelators Wang *et al.* has developed from the benzylidene acetal derivatives which saw gelation in organic and aqueous conditions (Figure 1.3).[12]

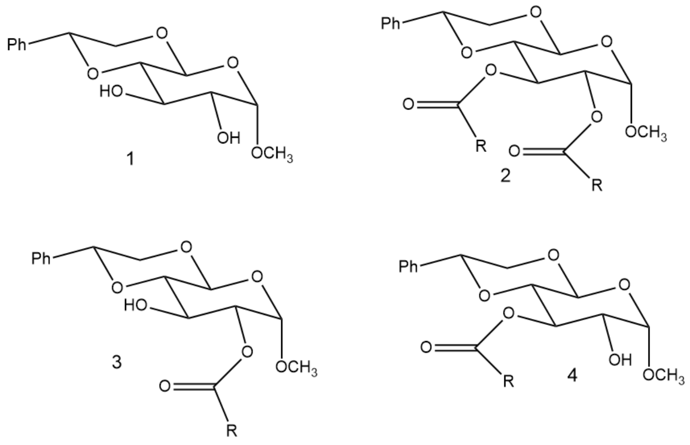

Figure 1.3: Structures of benzylidene acetal derivatives as LMWG's developed by Wang *et al.*[13]

One key attribute of LMWGs that has made them increasingly useful in modern applications is their high versatility and the responsiveness of the gels they form to external stimuli, owing to their structure being assembled via intermolecular forces, whereas polymer gels which involve many higher energy covalent bonds are much less responsive. Changes in temperature, pH or light can alter the gel's structure by disassembling the self-assembled network, meaning it can be utilised for use in a wide variety of applications.

1.3. Hydrogels in Transition Metal Catalysis

Hydrogels assembled by LMWGs and PGs have been finding increasing applications in the large field of transition metal catalysis. Transition metals are well known for their extensive use in catalysis owing to their large range of oxidation states and partially filled d-orbitals. However, their use in catalysis is complicated by the difficulty in their recovery to be reused for multiple chemical reactions. Many transition metals such as palladium and platinum are rare earth metals (the EU defined palladium as a critical resource material[14]) that are expensive and damaging to the environment to mine and refine into pure products for commercial use, and while catalysts are not used up in a reaction, their extraction during the work-up process can be time consuming and difficult, particularly for homogeneous systems. It therefore follows that recycling these catalysts so that they can be reused for multiple synthetic reactions is economically and environmentally advantageous.

The recycling of transition metal catalysts has therefore seen development using a wide range of methods. One method is by using liquid-liquid biphasic conditions to dissolve the catalyst and product in separate phases, making separation of the catalyst from products quick and easy. Theberge and coworkers designed a novel fluorous palladium ligand for Suzuki-Miyaura coupling that could be separated by dissolution in fluorinated solvents, while reagents and products were in the aqueous phase.[15] The fluorous solution containing the catalyst could then be added to the next reaction system. Immobilising a homogenous catalyst in solution is another method of catalyst recycling, and Leeuwen and coworkers demonstrated that a ruthenium catalyst used for enantioselective transfer hydrogenation could be immobilised *via* a covalent bond to a silica gel, which was packed into a glass column.[16]

Transition metal catalysts have therefore seen incorporation into hydrogels for recycling and increasing activity. Gels are particularly useful as catalyst supports because they can provide the advantages of both homogeneous and heterogeneous catalysts, with the high surface area of the fibrillar network, excellent solvent compatibility and easy separation of catalyst from products.[17] Metallogels are gels with transition metal catalyst complexes built into the structure of gels that could provide catalysts with large surface area and easy extraction, however the potential catalytic capability of these materials has not been broadly explored.[18] Fernandez *et al.* designed a palladium-coordinated complex that could gelate in aqueous conditions, although its catalytic potential has not been studied.[19] One of the few catalytic studies on catalytic supramolecular metallogels was done by Tu and co-workers, which used a bicarbene pincer palladium complex as a gelator that was used to catalyse a Michael addition in high yields (Figure 1.4).[20]

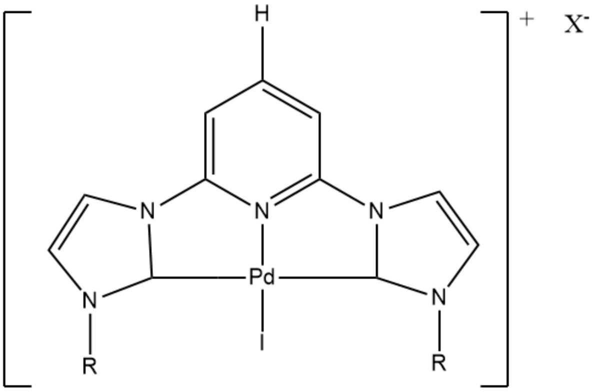

Figure 1.4: Biscarbene palladium complex metallogelator used for Michael addition, where R=$C_{16}H_{33}$

One type of heterogeneous transition metal catalyst are nanoparticles,[21] formed during the aggregation of metal atoms in solution by their reduction from a cation to a neutral state.[22] Some of the earliest work on catalytic nanoparticles was done by Hurata in 1986 on the use of gold metal oxide particles smaller than 5 nm for the oxidation of CO to CO_2. The nanoparticles were found to be 5 atom% Au and a 95% metal oxide (Fe_2O_3 or Co_3O_4) and could maintain high catalytic activity for 1 week.[23] More recent work on metal nanoparticles has extended into the field of organic catalysis.[24,25,26]

Research has now begun to show the growth and stabilisation of metal nanoparticles on/in a hydrogel support and further use for a wide variety of applications, including antimicrobial,[27,28] optical applications[29] and electronic conductivity.[30,31] Hydrogels are emerging as an ideal candidate for metal nanoparticle catalyst support as they are capable of preventing aggregation by immobilising the nanoparticles in the fibrillar network and additionally retaining the nanoparticles in their structure over time for repeated use. Nanoparticles are formed in hydrogels via the uptake of metal ions from the supernatant solution, which are then reduced within the gel (typically with the use of an additional reducing agent) to a neutral state. The metal atoms then aggregate together to form nanoparticles, which are unable to diffuse out of the gel because of the fibrillar network.

Maity and Maitra designed a calcium-cholate hydrogel that developed palladium nanoparticles with the addition of the reducing agent sodium cyanoborohydride, which could then catalyse Suzuki-Miyaura couplings in up to 99% yields at 90 °C and be reused up to four times (although catalyst activity and yields quickly depleted).[32] Firouzabadi *et al.* designed an agarose hydrogel that could reduce Pd(II) to Pd(0) using the hydroxyl groups on the polymer backbone, that was used for Mizoroki-Heck and Sonogashira couplings, and it was also capable of recycling the catalyst for multiple uses.[33] Finally, Li and co-workers developed a cellulose based hydrogel that bound Ni(II) and Cu(II) in solution, which could then reduce the metal ions to nanoparticles *in situ* with sodium borohydride. These nanoparticles were successfully used to catalyse the reduction of 4-nitrophenol to 4-aminophenol.[34] The nickel and copper nanoparticles gave 97% and 98% activity respectively, and even after 30 days in storage, the hydrogel-nanoparticle composites gave 70% activity.

Hydrogels potential to remove metal ions from solution can be further applied to treat wastewater contaminated with such species through diffusion into the gels, then aggregation of the ions into nanoparticles that are trapped within the fibrillar network. As metal nanoparticles supported on a hydrogel network have been demonstrated to catalyse a series of reactions, in principle this is a family of materials that can be used to provide strong environmental remediation and catalyst recovery, then further recycle them into highly active and stable metal catalysts. Further research into the multi-functional capabilities of these versatile hydrogels-nanoparticle materials can provide an excellent method of providing a green and sustainable method of transition metal catalysis.

1.4. DBS-CONHNH$_2$

DBS-CONHNH$_2$ is a supramolecular hydrogelator based on the well-known gelator 1,3:2,4-dibenzylidene sorbitol (DBS) (**1**) (Figure 1.5). DBS is a commercially available organogelator, but it has poor solubility in aqueous solution.[35] Derivatives of this LMWG have been developed in recent years to produce supramolecular hydrogels.[36] The two acyl hydrazide functional groups give DBS-CONHNH$_2$ (**3**) greater hydrophilicity, while the 2D shape of the molecular structure allows for π-π stacking and hydrophobic packing between the molecules, with additional hydrogen bonding between the alcohol groups on the aliphatic chain. DBS-CO$_2$H (**2**) is a closely related structure,[37] but gelates when protonated in acidic conditions, which makes it difficult to utilise for a wide range of chemical reactions. In contrast, gels formed by DBS-CONHNH$_2$ are stable over a pH range of 2-11.5 because of its acyl hydrazide groups, which have a pKa < 3.0.[38]

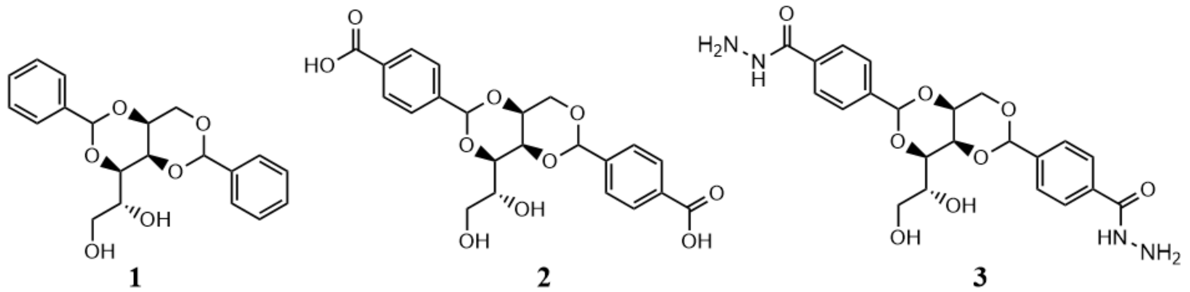

1 **2** **3**

Figure 1.5: 1,3:2,4- dibenzylidene sorbitol (**1**), DBS-CO$_2$H (**2**), DBS-CONHNH$_2$ (**3**)

DBS-CONHNH$_2$ has also been demonstrated to be capable of facilitating the formation and stabilisation of metal nanoparticles. Early research by Okesola *et al.* demonstrated that DBS-CONHNH$_2$ gels could be used to extract precious heavy metal ions ($Pd^{2+}/Ag^{+}/Au^{3+}$) from model waste water and further facilitate reduction to their neutral states, without the need for additional reducing agents. These atoms were then observed to aggregate into electrocatalytic nanoparticles, and TEM indicated they were located adjacent to the gel fibres.[39] This demonstrated that the DBS-CONHNH$_2$ was reducing metals and sterically stabilising the resulting nanoparticles in the gel matrix.

DBS-CONHNH$_2$ has been additionally demonstrated to allow these nanoparticles to be used in catalysis, although this has thus far been limited to palladium catalysis. Palladium nanoparticles grown *in situ* without the need for additional reducing agents, as seen in other examples[40] have been demonstrated by Slavik *et al.* to catalyse Suzuki-Miyaura,[41] Sonogashira and Heck reactions,[42] providing nearly full conversion to the intended products in aqueous conditions. These palladium-nanoparticle loaded hydrogels could further be recycled multiple times while maintaining high catalytic activity, before mechanical degradation of the gel prevented further recycles.

Additionally, silver nanoparticles in DBS-CONHNH$_2$ based gels have been used for *in vitro* antimicrobial applications by Piras and co-workers,[43] but their catalytic potential has not yet been studied. Silver nanoparticles in supramolecular and polymer hydrogels have seen previous use in the reduction of nitroaromatics to synthesise aniline and its derivatives, particularly 4-nitrophenol. Banerjee and co-workers used the tripeptide H$_2$N-ADDAPhe-Phe-COOH (ADDA: 12-amino dodecanoic acid) (Figure 1.6), a low-molecular weight hydrogelator that can gelate in either acidic or basic conditions (although not neutral conditions) to support silver nanoparticles, which were grown by reducing Ag(I) with the citric acid that is also used to assist in gelation.[40] The Ag nanoparticles were found to be bound to the LMWG fibres and also often in the spaces between (Figure 1.7). The silver nanoparticles were used to reduce 4-nitrophenol and 4-aminophenol as well as 4-nitroaniline to *p*-phenylenediamine in water, achieving very high conversion rates using sodium borohydride as a reducing agent.

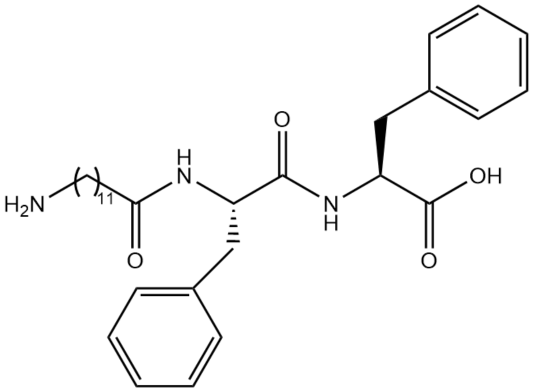

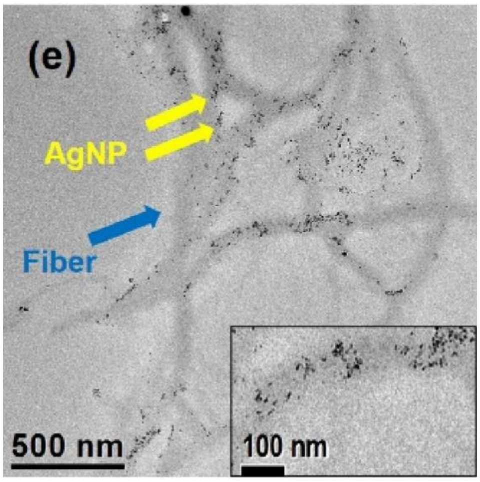

Figure 1.6 (left): Tripeptide low-molecular mass hydrogelator H_2N-ADDAPhe-Phe-COOH designed by Banerjee *et al.* used for silver-nanoparticle support
Figure 1.7 (right): TEM images by Banerjee *et al.* of gel fibres with silver nanoparticles bound to the fibres[40]

Similarly, Ghorbanloo *et al.* used a poly(acrylic acid) (p(AA)) hydrogel as a silver nanoparticle scaffold.[44] These nanoparticles were grown via Ag(I) ions in solution binding to the gel fibres, then reduced to Ag(0) with sodium borohydride (Figure 1.8). These nanoparticles were then used to catalyse the reduction of 4-nitrophenol with sodium borohydride, as well as the oxidation of benzyl alcohols with oxygen. The recyclability of the p(AA)-Ag system for the oxidation of benzyl alcohols was also tested and found to maintain high catalytic activity for 3 repeats.

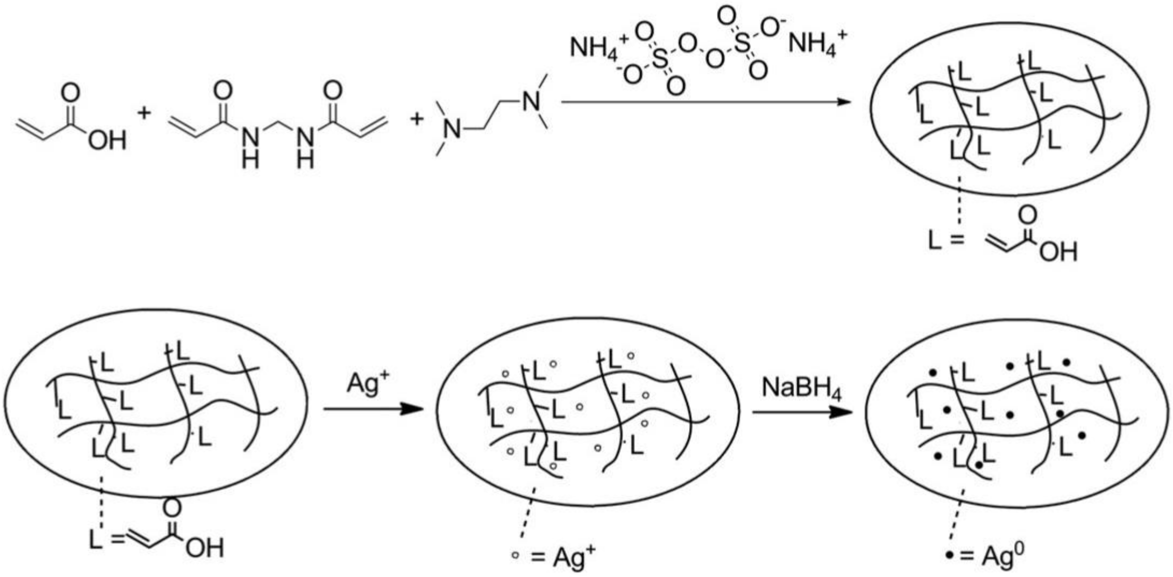

Figure 1.8: Cross-linking of p(AA) and formation of silver nanoparticles as described by Ghorbanloo[44]

Furthermore, very little research has studied the catalysis of hydrogels loaded with multiple different metal nanoparticles, so that a single hydrogel can be used for an even larger pool of reactions, such as combining silver with palladium nanoparticles to provide the both well researched Suzuki-Miyaura couplings and the nitroarene reduction. A single species that is easy to prepare and handle, that can catalyse a large variety of reactions and be recycled while additionally retaining high activity could be a very powerful technology.

1.5. Hybrid Hydrogels

LMWGs, including DBS-CONHNH$_2$, form rheologically weak gels as they are assembled by low-energy intermolecular forces, so the gels are easily damaged and difficult to handle. However, they can be combined with polymer gels (PGs), which are much stronger than supramolecular gels owing to the large number of covalent bonds that make up their structure. These make hybrid gels, which combine the highly versatile nature of LMWG's with the strength of polymer gels.[45]

Feng and co-workers designed a hybrid hydrogel by merging the LMWG 1,4-bis(phenylalanine-diglycol)-benzene (PDB) with the PG sodium alginate, which was used for controlled model drug release.[46] The addition of the PG to PDB gave a hybrid gel that retained the drug release abilities of PDB while improving mechanical strength. Sodium alginate also improved the water retention abilities of the LMWG, and introduced electrostatic interactions which aided selectively.

Nowak and Ravoo more recently developed a peptide LMWG that was combined with the polymer gelator agarose.[47] The peptide LMWG, AAP-FGDS, could disassemble in UV light and reassemble in visible light. Combining this with agarose gave a two-component hybrid hydrogel that could have one fibrillar network disassemble and reassemble while the other self-supporting network remains intact.

DBS-CONHNH$_2$ has also already been combined with both agarose and sodium alginate. Viera *et al.* used agarose to increase the robustness of the LMWG in a heparin release study. This only marginally reduced the rate of release when compared to the DBS-CONHNH$_2$-only gel, and also allowed it to be shaped in a standing cylinder to increase surface area, greatly increasing the heparin release from 62% to 90%.[48] Piras and Smith designed a DBS-CONHNH$_2$ and sodium alginate hybrid gel, which was used to spatially resolve the hydrogel into beads to increase surface area.[49] The beads were then loaded with palladium nanoparticles to catalyse Suzuki-Miyaura cross-couplings in up to 99% yields within 24 hours.

Hybrid gels can be further spatially resolved into formal shapes, including small beads as previously reported by Piras *et al.* The polymer gelator chosen for this purpose was based on sodium alginate, which can be added dropwise to CaCl$_2$ solution to give small "beads". Alternatively, agarose can be made into similarly sized beads by adding dropwise to cold, apolar solvents, which could propel through water when loaded with ethanol due to the Marangoni effect.[50]

1.6. Aims and Objectives

We therefore envisage the use of hybrid hydrogels in catalysis, specifically both the DBS-$CONHNH_2$/sodium alginate and DBS-$CONHNH_2$/agarose gel beads by embedding transition metal nanoparticles. Nanoparticles will be characterised with respect to their size and location using TEM, and catalyst loading per bead will be determined using UV-VIS for palladium-nanoparticle beads, and titrations with NaCl for silver-nanoparticle beads.

Palladium has been previously studied on a DBS-$CONHNH_2$ support, and we therefore wanted to explore if other precious metal nanoparticles could catalyse a series of reactions within the same framework. With this target in mind, we will study silver nanoparticle loaded gel beads as the catalyst, investigating the reduction of 4-nitrophenol to 4-aminophenol, using $NaBH_4$ in an aqueous medium.

This scope will then be expanded to the isometric nitrophenols and further nitroarenes to study the selectivity of the catalyst, with yields calculated using ^{1}H NMR. Furthermore, we will explore the recyclability of the bead species for the reduction of 4-nitrophenol and attempt to optimise the conditions to maximise the number of recycles.

Additionally, we will look to embed palladium and silver nanoparticles into both bead species, then look to apply both nitroarene reduction and Suzuki-Miyaura cross-coupling onto the same molecule to provide a one-pot, two-step synthesis of a desired product.

These orthogonal processes can potentially be optimised by combining the two hybrid hydrogels into one, and producing a hydrogel embedded with multiple metal nanoparticle species. We will look to do this by developing a single bead species with both palladium and silver nanoparticles grown within a single gel bead, and catalyse both a 4-nitrophenol reduction and Suzuki-Miyaura cross-coupling of 4-iodophenol with phenylboronic acid. If such a system can work, then we will have developed a tool for catalysing a broad range of reactions that is easy to produce and handle and can potentially be recycled.

In the longer term, we envisage these catalyst-loaded gel beads may have applications in the development a commercially available easy-use catalyst kit, whereby chemists would be able to simply add beads to a reaction system. This would negate the need for time-consuming and expensive set-up of catalysts, while also making their removal during the work-up much simpler than using aqueous catalysts. Furthermore, a catalyst support that is easy to recycle for multiple series of reactions can provide a green method for reusing precious metals, with no need for a work-up with potentially environmentally hazardous species.

1. RESULTS AND DISCUSSION

1.1. Gel Beads

1.1.1. DBS-CONHNH$_2$ Synthesis

1,3:2,4-Di(4-acylhydrazide)benzylidene-D-sorbitol (DBS-CONHNH$_2$) was synthesised in two steps from the commercially available D-Sorbitol, a sugar obtained from the reduction of glucose, and two equivalents of 4-methyl carboxybenzaldehyde. The first step involved a condensation reaction under Dean-Stark conditions to synthesise DBS-CO$_2$Me, using *p*-TsOH as an acid catalyst and a 7:3 mix of cyclohexane and methanol as solvent. The condensation involves a double cyclisation between the alcohol groups of D-sorbitol and the aldehyde of 4-methyl carboxybenzaldehyde. The reaction was run at 70 °C for 3 hours, after which a white insoluble precipitate is formed in the reaction mixture. The solid was then washed with methanol, then refluxed in water (100 ml for 3 x 30 mins), and DCM (100 ml for 3 x 30 minutes), and finally left to dry on a Büchner funnel over vacuum. This gave a 26% yield of the desired product, a white solid (Figure 2.1.1).

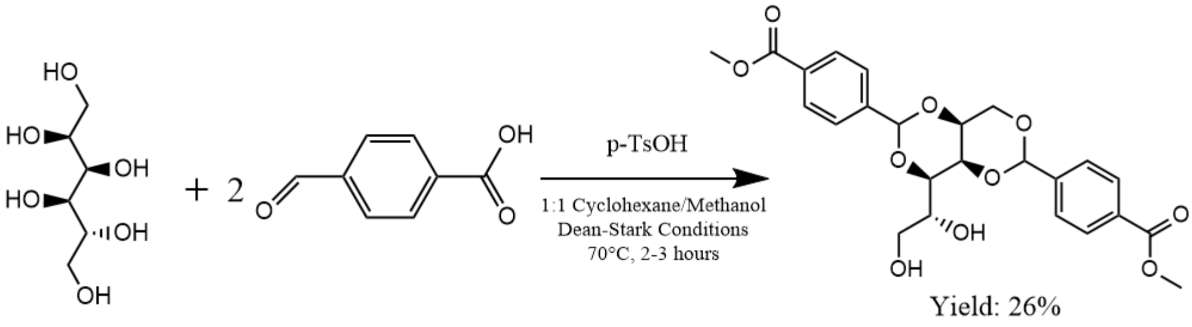

Figure 2.1.1 - Synthesis of DBS-CO$_2$Me

DBS-CONHNH$_2$ was synthesised in the second step from DBS-CO$_2$Me using hydrazine monohydrate in THF in an overnight reflux. The mixture was then washed with water, then dried in a vacuum oven for 4 hours until the powder was fully dry, when the mass remains unchanged after further drying in the oven. This gave DBS-CONHNH$_2$ in 89.5% yield (Figure 2.1.2). Confirmation of the synthesis of DBS-CO$_2$Me and DBS-CONHNH$_2$ was done by ^{1}H NNMR spectroscopy, and comparison with spectra taken by Okesola indicated the formation of both products.[38]

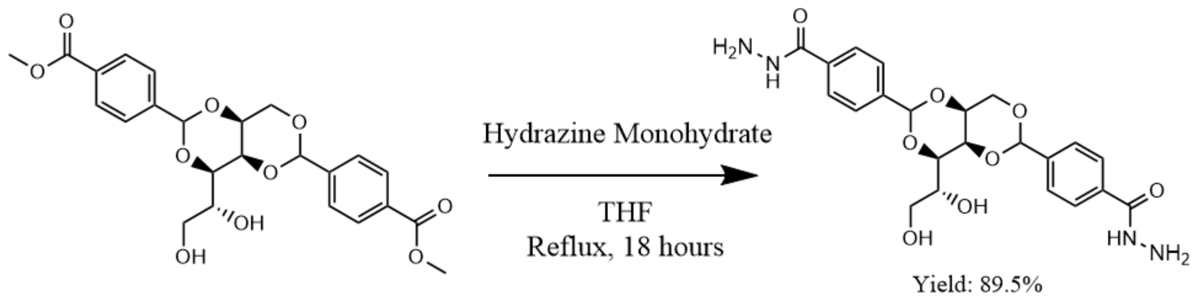

Figure 2.1.2 - Synthesis of DBS-CONHNH$_2$

1.1.2. Gel Formation

DBS-CONHNH$_2$ is a hydrogelator that forms gels in water at a loading of 0.3% wt/vol. The gel assembles by application of a simple heat-cool cycle, where the suspension is heated until the complete solvation, in which state the individual DBS-CONHNH$_2$ molecules can form the fibrils while cooling, resulting in gelation. The gel is translucent white in appearance, and is also mechanically soft on its own, making it very difficult to handle outside of the vial in which it is formed.

Due to its soft nature, DBS-CONHNH$_2$ can be combined with polymer gels (PG) to strengthen it. Sodium alginate is a commercially available gelator that is derived from brown algae, which gelates when added to calcium chloride by cross-linking two polymer chains together. The combined gel of DBS-CONHNH$_2$ with calcium alginate can be spatially organised into specific shapes to emphasise specific properties, such as increasing surface area to improve the rate of diffusion. Gel 'beads' are one example, that encapsulate a core-shell structure with the PG (sodium alginate) as the shell, providing a robust mechanical strength, and the LMWG as the core giving the bead its unique properties. In this way, the PG can be considered to act as a mould or 'chemical reaction vessel' to control the self-assembly of the LMWG.

Initially, we produced only beads, made with 0.3% wt/vol of DBS-CONHNH$_2$ and 0.75% wt/vol sodium alginate in water. The DBS-CONHNH$_2$ was added as a solid, while the sodium alginate was added from a premade solution. After sonication for 15 minutes, the suspension was heated until full solvation, after which the solution was added dropwise to 5% wt/vol CaCl$_2$, which would form the beads on impact as the alginate cross-links. Initial attempts at making the beads did not produce the spherically shaped beads hoped for, but instead wide and flat gels that did not hold their shape. These offered much less stable gels (they could tear more easily) and were not as easy to handle and move to different vials.

The process for formation was optimised to produce beads of more consistent size and shape. It was recognised that adding the beads dropwise while the solution was still hot (just after dissolving the DBS-CONHNH$_2$ and alginate) would give the wide and flat beads. This is because adding the gel solution while still hot, and therefore more liquid-like, means it cannot hold its shape when hitting the water surface, giving the wide and flat shape.

Furthermore, heating the suspension too much could decompose the sodium alginate, which may also give the less stable disc-shaped beads. To resolve this, heating was stopped immediately after solvation, after which the gel was allowed to cool until gelation had begun (to the point where it could be inverted) before adding dropwise to the CaCl$_2$. This allowed for a more consistent bead size and shape, with a typical size of 3 mm diameter. Assuming a spherical shape, this gives a volume of 14.1 mm^3.

In experiments involving the reduction of aromatic nitro-compounds using $NaBH_4$ (discussed more extensively in Section 2.1.1), it was found that the DBS-$CONHNH_2$/alginate beads would easily fragment in the presence of $NaBH_4$. We therefore decided to use hybrid hydrogel beads with the polymer gelator agarose instead of alginate to potentially improve stability.

Agarose is a polysaccharide extracted from red seaweed, which cross-links into a polymer gel in a heat-cool cycle, similar to DBS-$CONHNH_2$. The DBS-$CONHNH_2$/agarose gel beads are made up from 0.3% wt/vol of the LMWG and 1% wt/vol of the PG, which was suspended in water and sonicated for 15 minutes. This suspension was heated until complete dissolution of both components, which was then added dropwise to cold paraffin oil. The paraffin oil was washed in three steps by consecutive submersion in petroleum ether (30 minutes), ethanol (30 minutes) and finally water (30 minutes). While the paraffin oil does require multiple steps to clean off the beads, it is used rather than cold water as the beads will lose their shape before gelation when added in while still hot. In contrast, the apolar paraffin oil forces the hydrogel to maintain its spherical shape until they are robust enough to hold the bead structure over time.

The agarose-based beads had a larger range of sizes when compared to the alginate-based beads. This was due to the timing of the addition of the droplets; the agarose solution is added hot and so is not viscous, whereas the alginate solution was added while partially gelated, and so was more solid-like. As a result, the droplets of the alginate solution are much easier to control in size, hence the volume of the eventual alginate-beads have a greater consistency relative to the agarose beads.

The DBS-$CONHNH_2$/agarose beads offered much more stability in the presence of $NaBH_4$ than the DBS-$CONHNH_2$/alginate beads; the fragmenting of beads in the alginate-based beads was not observed in the agarose-based beads, which maintained their shape and structural integrity.

2.2. Silver Nanoparticles

2.2.1. Uptake of Ag^+

Nanoparticles are formed in solution by the reduction of metal cations to neutral metal atoms, which then aggregate together into the nanoparticles. Many LMWGs require the use of an additional reducing agent to produce the metal atoms, such as citric acid. However, DBS-CONHNH$_2$ is capable of reduction due to its hydrazide wings acting as reducing agents, and then further stabilising the nanoparticles to terminate growth.

Formation of silver nanoparticles in DBS-CONHNH$_2$ based gels was done by submerging the gel in a solution of Ag^+, where after a minimum of three days the nanoparticles were able to grow inside the gel matrix. Ag^+ forms an insoluble white precipitate with Cl^-, and as the DBS-CONHNH$_2$/alginate beads require $CaCl_2$ to cross-link the alginate, the beads must be thoroughly washed before addition to the Ag^+ solution. This is done by immersing the beads in water and giving time (1-3 days) to allow the Cl^- ions to diffuse out of the beads, replacing the water regularly.

The uptake of Ag^+ by the beads was measured via titration of the supernatant with 0.05 mM NaCl and 5% wt/vol potassium chromate to determine the molar quantity of silver that each bead had taken in. Silver ions preferentially form a precipitate with chloride ions over chromate (which gives a red precipitate with silver), so small concentrations of NaCl can be titrated, and the red colour of the silver chromate gives an end point to the titration. The calculated concentration of Ag^+ remaining in the supernatant will therefore give the number of moles incorporated into the beads.

The beads typically took in between 0.1 and 0.5 μmol of Ag^+ as calculated using titrations. Considering that later nitro-arene reductions would use 0.216 mmol of compound for a reaction, this gives a catalyst loading of approximately 0.04 - 0.23 mol% per bead, meaning using 10 beads could typically give approximately 1 mol% of catalyst for a reaction.

After the nanoparticle growth and formation was completed in the beads following three days in the $AgNO_3$ solution, the colour of the beads changed from a translucent white to a reddish brown. The darker brown colours indicated the full reduction of Ag(I) to Ag(0), with Ag(I) giving colourless beads. The colour of the beads comes from the surface plasmon resonance bands that are given off by the nanoparticles. Often white spots were present on the beads, which was likely due to residual Cl^- forming the insoluble precipitate with Ag^+ if they were not washed fully.

We also used Transmission Electron Microscopy (TEM) to view the nanoparticles on the nanometre scale (Figure 2.2.1).

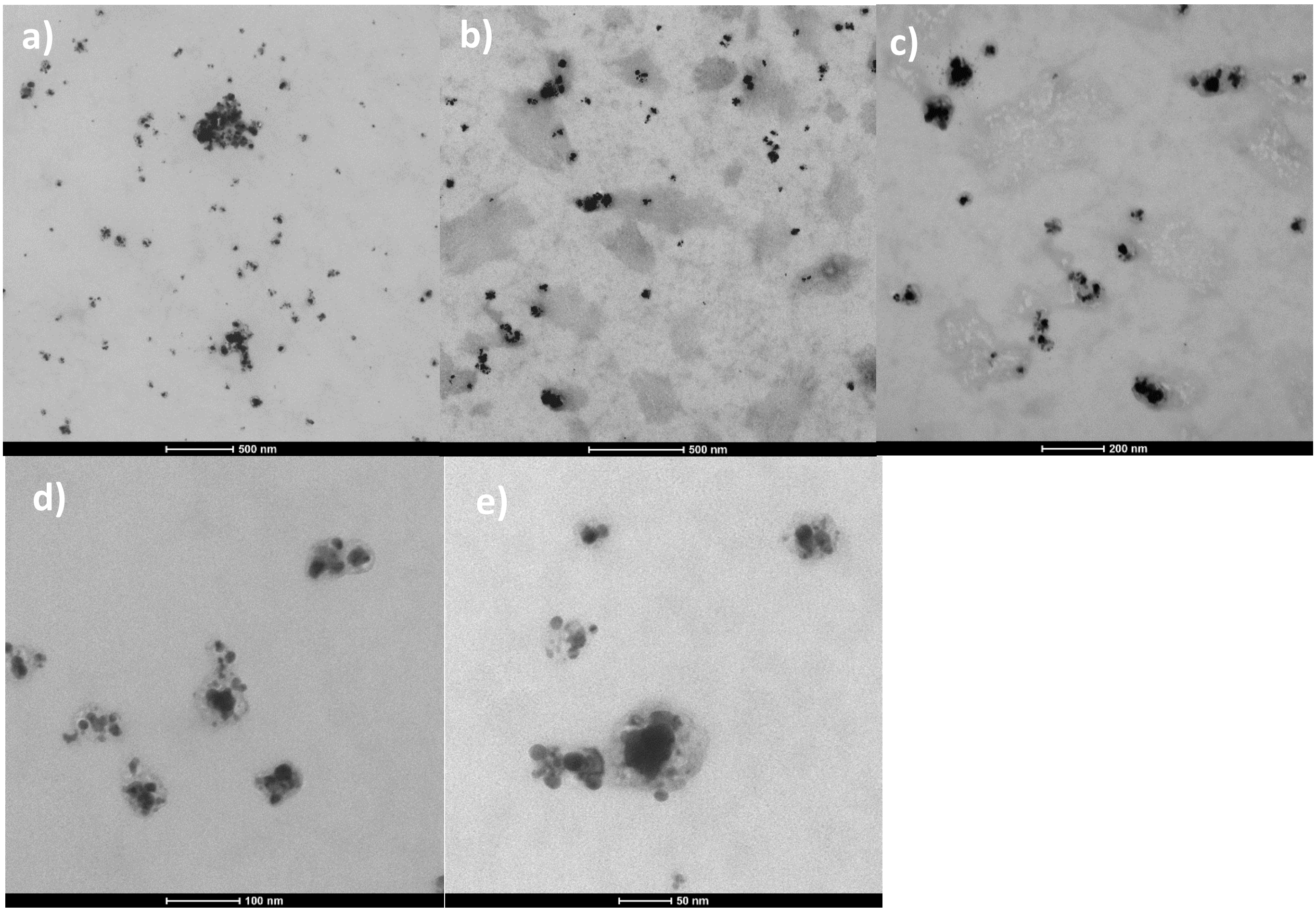

Figure 2.2.1. (a)-(e): TEM Images of DBS-CONHNH$_2$/sodium alginate gel beads loaded with silver nanoparticles. Scale bars (a) and (b) 500 nm; (c) 200 nm; (d) 100 nm; (e) 50 nm

The dark black spots demonstrated the presence of nanoparticles forming in the gel, as they strongly absorb the electrons. The TEM images suggested that the silver nanoparticles were regular in size and typically spherical in shape, although some aggregation of groups of nanoparticles had occurred. The average size of the nanoparticles measured about 20-50 nm, which was significantly larger than silver nanoparticles previously reported to be produced in DBS-CONHNH$_2$.[43]

2.2.2. Catalytic Studies

A common use for silver nanoparticles is in catalysis, and notably for the reduction of aromatic-nitro compounds. 4-nitrophenol is an intermediate in the synthesis of paracetamol, which must be reduced to 4-aminophenol as one of the steps, and we therefore first tested our beads to reduce 4-nitrophenol (4-NP) to 4-aminophenol (4-AP). The alcohol functional group allows 4-NP to dissolve easily in water, so it can diffuse into the gel to interact with the nanoparticles. 4-NP and 4-AP are additionally both low hazard materials, making multiple experiments with them low risk.

The reduction of 4-NP is carried out with $NaBH_4$, which is a cheap, commercially available reducing agent. $NaBH_4$ decomposes in water, the solvent most commonly used in the nitro-reductions, which meant that $NaBH_4$ had to be added in large excess so that a sufficient amount could be used to reduce the nitro-group. $NaBH_4$ was added in 10x molar excess to provide enough BH_4^- to successfully reduce the nitro group. Previous research by Kong *et al.* has demonstrated that although the reduction without the presence of a catalyst is thermodynamically favourable, the reaction will not occur, even with a molar excess of 4-NP:$NaBH_4$ of 1:100 and a reaction time of one week.[52]

Our first attempt at reducing 4-NP used 5 ml of water as the solvent, ran at room temperature and for 3 hours total (Figure 2.2.2). The dissolution of 4-NP gave the mixture a weak yellow colour at 399 nm, then the addition of $NaBH_4$ gave a much stronger yellow, as well as effervescence from the evolution of hydrogen gas from the degrading $NaBH_4$, which had to be released regularly from the vial. The alginate-based beads additionally turned a black colour and began fragmenting into smaller particles. Over the three hour reaction time, the mixture changed from a strong yellow to a dark grey, with the beads' structural integrity mostly destroyed.

The product was extracted with ethyl acetate and washed with 1 M $NaOH_{(aq)}$, yielding a grey solid, which was analysed by ^1H NMR spectroscopy. This indicated a high conversion to 4-aminophenol, with 68% overall yield.

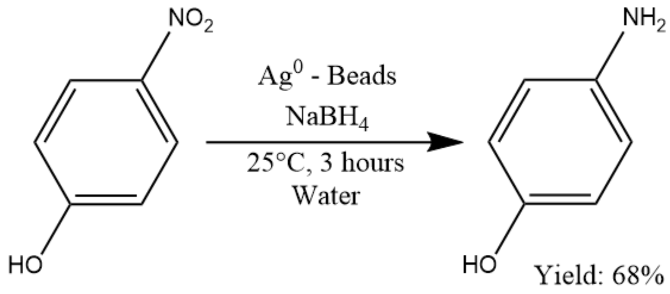

Figure 2.2.2 - 4-nitrophenol reduction to 4-aminophenol

After the successful reduction of 4-nitrophenol, we looked to expand the scope of the reaction to encompass a wide range of nitro-aromatic compounds. Initially we looked at the rest of the nitro-phenol isomers, 3-nitrophenol (3-NP) and 2-nitrophenol (2-NP) which were also soluble in water and may reveal information about the regioselectivity of the process.

The reaction conditions, length and molar quantities were kept the same as with the 4-NP reduction.

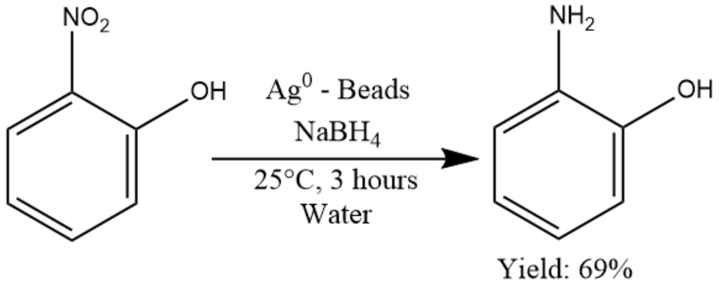

Figure 2.2.3 - 2-nitrophenol reduction to 2-aminophenol

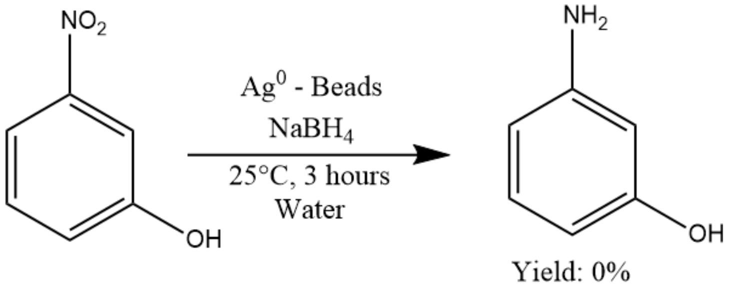

Figure 2.2.4 - 3-nitrophenol reduction to 3-aminophenol

2-NP formed a weak yellow colour when added to the reaction mixture and gave a golden brown when $NaBH_4$ was added (as it initially deprotonates the alcohol group). After 3 hours, the solution had gone clear in colour, similarly to the 4-nitrophenol reduction, indicating a successful reaction had taken place, while the beads had also darkened in colour and significantly fragmented in the presence of the $NaBH_4$.

The mixture was filtered on paper to remove the bead particles, and the product was then extracted with ethyl acetate, which was dried and concentrated, yielding a pink solid, with a yield of 69%. The product was analysed by ^1H NMR spectroscopy, which showed evidence of ethyl acetate and starting material still present in the sample, meaning that the actual yield was likely lower.

We then tested the 3-nitrophenol reduction by the silver-nanoparticle gel beads, which forms an orange colour when dissolved in the solvent, turning a stronger golden colour when $NaBH_4$ was added. As with 2- and 4-NP, the same reaction conditions were kept the same throughout, with water as the solvent, room temperature and a three hour reaction time. After the three hours, the solution went clear, however when the vial was opened and exposed to air the solution quickly turned a strong dark red colour again. This reduction was performed multiple times and this phenomenon was observed each time, and ^1H NMR spectroscopy did not indicate the formation of any product.

Following the reduction of the nitrophenols, we looked to reduce a broad range of substituted nitro-arenes. The primary issue with reducing many of these compounds is that they are typically hydrophobic because of the aromatic ring, particularly those with additional non-polar groups substituted onto the ring. Because of this, it was difficult for many compounds to be dissolved in water and diffuse into the gel beads to make contact with the silver catalyst.

Table 1: Nitro-arene reduction with $NaBH_4$

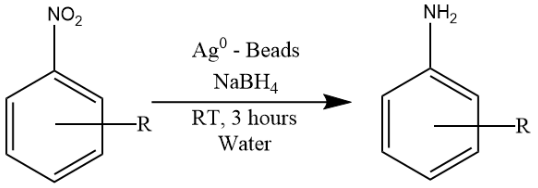

Reagent	Product	Yield
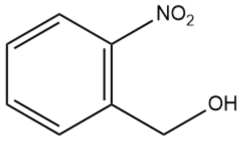	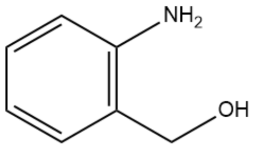	Returned starting material
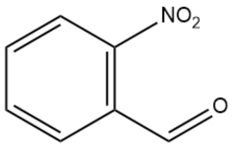	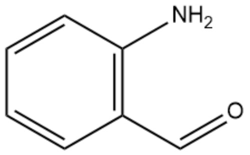	Returned starting material
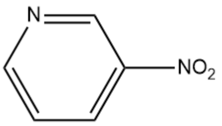	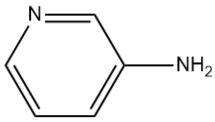	Returned starting material
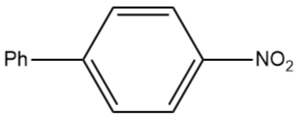	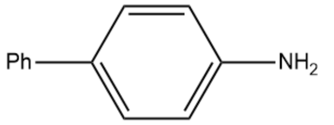	Returned starting material
		Returned starting material
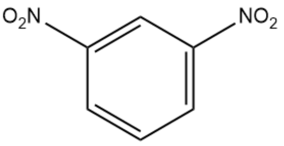	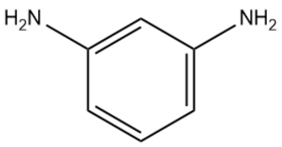	Returned starting material
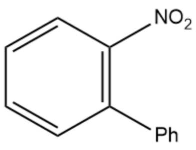	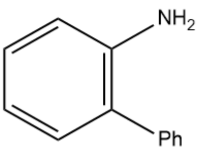	Returned starting material

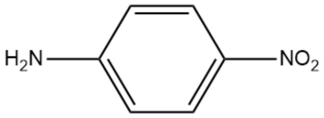	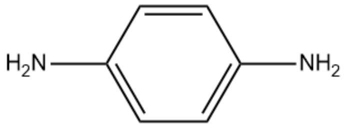	Returned starting material

2.2.3. UV-Vis Studies

We then tested the change in UV-Vis absorption over the reaction period for the 4-nitrophenol, 3-nitrophenol and 2-nitrophenol, in order to determine the rate of reaction and observe how the position of each nitro-group affects the mechanism. Due to the strong colour of the phenols, the samples were heavily diluted so the spectrometer could properly measure the absorbance.

Upon addition of $NaBH_4$, we saw an initial peak at approximately 399 nm, giving the strong yellow colour, which corresponded to the 4-nitrophenolate ion, as $NaBH_4$ deprotonates the acidic aromatic alcohol. This began to drop over time, with a second peak at 297 nm beginning to rise from the second reading, which corresponds to the formation of 4-aminophenol. This peak is outside the visible spectrum of light, so no colour change of the solution occurred.

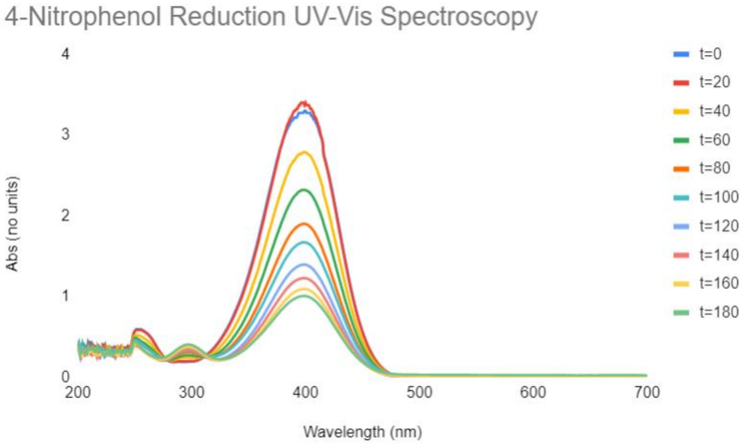

Figure 2.2.5 – UV-Vis Spectroscopy of 4-Nitrophenol Reduction

2-nitrophenol was also studied using UV-Vis spectroscopy, which saw similar results to 4-nitrophenol (Figure 2.2.6). The initial peak at 413 nm quickly drops after the addition of $NaBH_4$, followed by a rise in the peak at 288 nm, indicating the formation of 2-aminophenol over the reaction period.

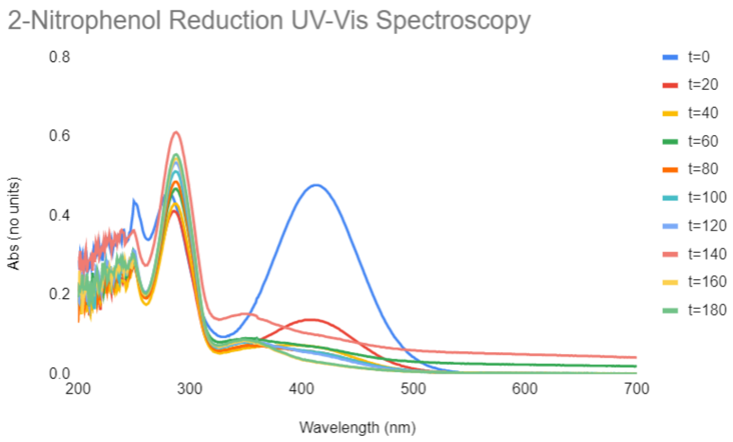

Figure 2.2.6 – UV-Vis Spectroscopy of 2-Nitrophenol Reduction

The 3-nitrophenol reduction however does not display any evidence of a reaction occurring, as once the 3-nitrophenolate peak at 399 nm is formed, there was no significant change in the peak absorption over the three hours (Figure 2.2.7). This indicates that there was no formation of the intended 3-aminophenol product.

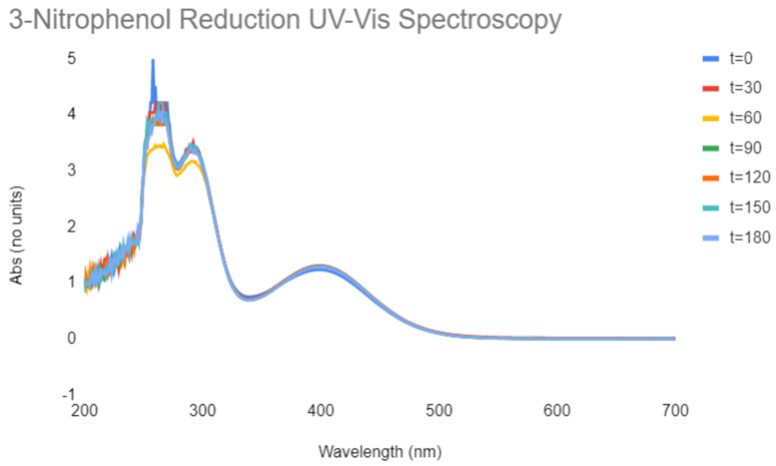

Figure 2.2.7 – UV-Vis Spectroscopy of 3-Nitrophenol Reduction

From the UV-Vis data, the rate of reaction for both the reduction of 2-nitrophenol and 4-nitrophenol could be determined. Due to the large excess of $NaBH_4$ used in both reductions, the concentration of sodium borohydride can essentially be considered constant, the reactions could both be considered pseudo first order with respect to the substrate,[51] giving a rate equation of

$$\ln\left[\frac{A_t}{A_0}\right] = -kt$$

where A_t is the concentration at time t, A_0 is the initial concentration, and k is the rate constant. Therefore, -k is equal to the slope of the line of $\ln(A_t/A_0)$ vs t. The rate constant k for the 4-nitrophenol reduction was calculated to be 6.8×10^{-3} min^{-1}, while for the 2-nitrophenol reduction was 1.9×10^{-2} min^{-1}.

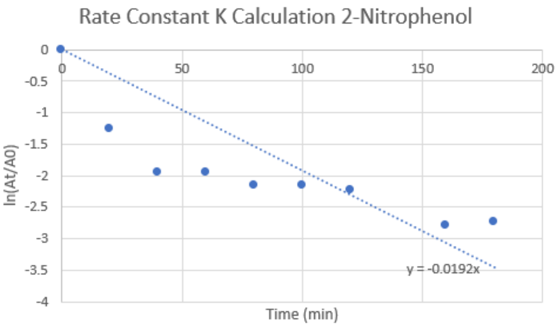

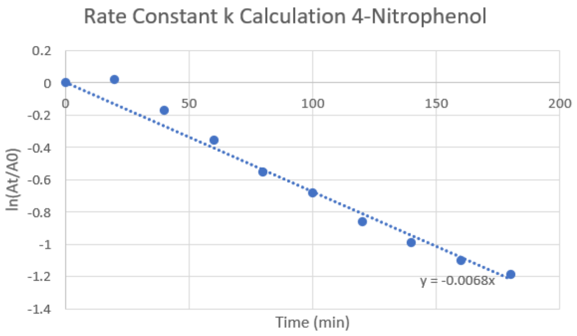

Figure 2.2.8 (Left) – Plot of ln(A_t/A_0) against reaction time for 2-nitrophenol
Figure 2.2.9 (Right) – Plot of ln(A_t/A_0) against reaction time for 4-nitrophenol

The results indicate that the mechanism of the nitro reduction does not occur when at the meta position, likely because the two substituents of 3-nitrophenol cannot provide the same mesomeric effect as in 2- and 4-nitrophenol. As the rate constant k is directly proportional to the rate of reaction, the calculated constants suggest that 2-nitrophenol reduces at a faster rate than 4-nitrophenol. However, it should be noted that for 2-nitrophenol, the fitting to first order kinetics was particularly poor and therefore, although the reaction is clearly significantly faster, this rate constant should not be considered robust.

2.2.4. Recyclability Tests

One of the primary purposes of using the DBS-CONHNH$_2$ beads to support transition metal catalysts is to easily recycle the metals for multiple uses. This removes the need for a potentially time consuming and difficult extraction process of the catalyst during the work up, whereas removing the beads merely requires the use of a pair of tweezers. The aim would be to determine how often the silver-nanoparticle DBS-CONHNH$_2$/alginate beads could be recycled over a series of reactions (namely, the 4-nitrophenol reduction to 4-aminophenol), while both examining how the yield of each consecutive reaction changes and observing how the structural integrity of the beads is maintained.

The series of reactions were performed to the same protocol as the initial 4-nitrophenol reductions, using the large 10x molar excess of NaBH$_4$. The amount of sodium borohydride used would be the largest factor in how many times the beads could be recycled, as it was the reagent causing significant degradation of the DBS-CONHNH$_2$/alginate beads during the reaction process.

The DBS-CONHNH$_2$/alginate beads were difficult to recycle, not due to the silver catalyst but because of the large amount of mechanical degradation from the beads. Following the first reaction, the beads had significant fragmentation, particularly if the vial was disturbed (such as by lightly shaking to disperse the reagents). The smaller fragments were unable to be recovered using tweezers or a small spatula and so were removed in the work up using filter paper and discarded. Following the second recycle, there appeared to be no gel beads remaining in the vial and a small collection of fragments on top of the solvent. This indicated that the hydrogel structure had collapsed entirely, owing to the fact that there appeared to be much less overall volume of hydrogel present in the sample than was initially added.

Attempts to optimise the recycles to retrieve a larger number of iterations did not achieve much more success. As $NaBH_4$ was the component causing significant degradation of the beads, we reduced 4-nitrophenol with 5 times, 2 times and the molar equivalent of $NaBH_4$ present. This would ideally result in much less fragmentation of the beads, giving several extra recycles as structural integrity could be retained, as catalytic activity was not appearing to have been lost in the presence of $NaBH_4$.

In all three tests, only one recycle was possible. In both the 5 and 2 equivalents tests, the beads were almost entirely destroyed after 1 recycle (giving two total reductions) and therefore could not be recovered for an additional recycle, and in the case of the molar equivalent the reduction did not progress to completion in the first recycle, despite the beads remaining largely intact.

The DBS-$CONHNH_2$/alginate beads did not overall display significant ability to be used for multiple recycles of the 4-nitrophenol reduction, even when the quantity of sodium borohydride was greatly reduced to the molar equivalent of 4-nitrophenol. The mechanical degradation of the beads in the presence of $NaBH_4$ greatly hindered any repeat runs, making it difficult to transfer the beads between reaction systems, or destroying them during the reaction time so that none could be salvaged.

2.3. Palladium Nanoparticles

2.3.1. Uptake of Pd^{2+}

As well as reducing silver to a neutral state, DBS-CONHNH$_2$ is additionally capable of reducing Pd^{2+} ions to its atom Pd^0. Palladium nanoparticles can catalyse a large variety of reactions, most commonly the Suzuki-Miyaura cross-coupling which is widely used in the pharmaceutical industry.[53]

Uptake of palladium into the DBS-CONHNH$_2$/alginate beads was achieved by submersion into a solution of 5 mM $PdCl_2$, which was dissolved in 0.5 M HCl, after which the beads were left for at least three days to allow time for nanoparticle formation. Following this period, the beads were a light orange colour, with their size unchanged. There was a notable volume of small particles suspended in the $PdCl_2$ solution (Figure 2.3.1).

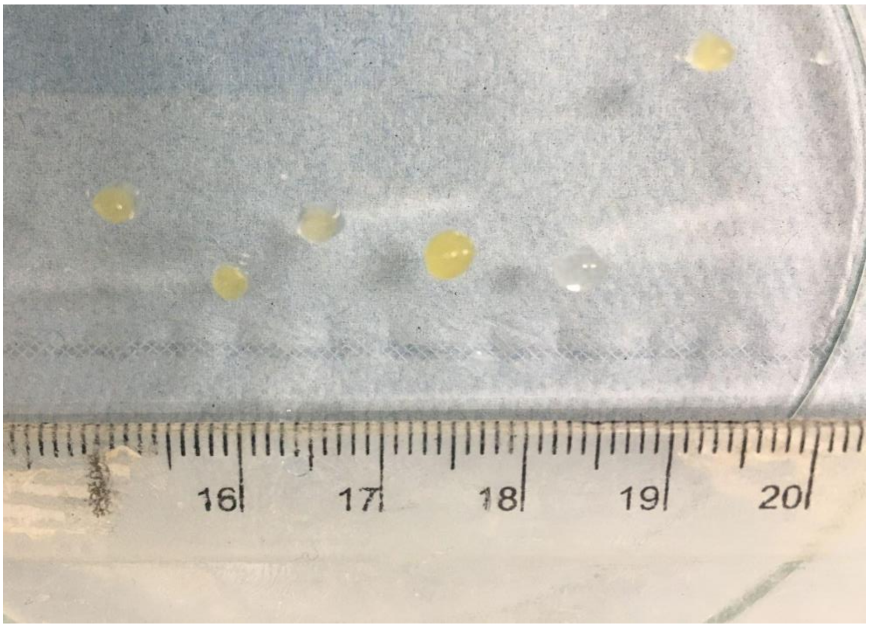

Figure 2.3.1 - DBS-CONHNH$_2$/Alginate Beads loaded with Pd

The quantity of palladium that had diffused into the beads was determined by UV-Vis spectrometry by measuring the absorption of the Pd^{2+} supernatant before and after the given period for nanoparticle formation. Pd^{2+} has a peak at 472 nm which gives the solution its orange colour, so a calibration curve would give the quantity of Pd^{2+} left in the sample, and therefore the quantity in each individual bead (Figure 2.3.2). The typical molar quantity of Pd taken up by individual beads was calculated to be 0.046 mmol per bead on average.

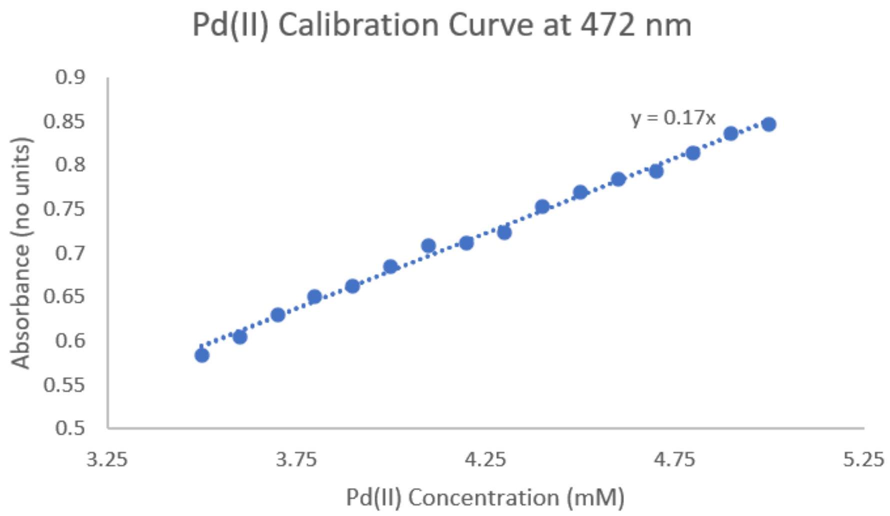

Figure 2.3.2 – Calibration curve of Pd(II)$_{(aq)}$ at 472 nm

The palladium-loaded beads were first tested for their catalytic activity in a Suzuki-Miyaura coupling between 4-iodotoluene and phenylboronic acid. This type of reaction was previously tested by Smith and co-workers for Pd-loaded beads.[49] This method utilises K_2CO_3 as the base required for the reaction. 3:1 ethanol/water was used as a solvent; this provides a sufficiently hydrophilic system for the beads while also allowing more hydrophobic compounds to dissolve and diffuse into the beads.

The reaction was run at 50 °C for 24 hours using 22 total beads. When K_2CO_3 was added to the solution (added last), the beads turned a brilliant orange colour, after 24 hours the solution remained unchanged in colour. The palladium-loaded beads were easily removed with tweezers and discarded. The product was extracted with diethyl ether and washed with 1 M NaOH$_{(aq)}$ and analysed with ^{1}H NMR spectroscopy. Unfortunately, no evidence of product formation was observed by ^{1}H NMR spectroscopy.

Two more attempts were made at the same reaction, but no success was found in trying to couple the two aromatics together. The second and third attempts used 15 and 24 beads respectively, in the same conditions and equal reagent quantities. The beads after the given reaction time were found to go dark brown in colour, with the solution clear. Both times, the product was extracted with ethyl acetate and washed with 1 M NaOH$_{(aq)}$ and analysed by ^{1}H NMR spectroscopy.

We initially suspected that the failure of the reaction was due to the low solubility of 4-iodotoluene in the 3:1 ethanol/water solvent, and that there was no diffusion of the coupling reagent into the beads to the catalyst site. We then attempted to combine the silver and palladium nanoparticle beads into a one-pot synthesis, with two orthogonal catalytic processes (the nitro-reduction and Suzuki-Miyaura cross-coupling) occurring at the same time. The beads should prevent interactions between the two catalytic sites while remaining in the same system, allowing the reagents to travel between the catalytic sites.

The orthogonal reaction would require an aromatic molecule both with a nitro-group to be reduced and a halide to couple with phenylboronic acid, so we used 4-nitroiodobenzene as the reagent of choice. To first test the feasibility of the one-pot synthesis, we probed each individual process on the 4-nitroiodobenzene separately, which may help discover what conditions may need to be required.

The reduction of the 4-nitroiodobenzene with the use of silver-nanoparticle loaded beads is extensively discussed in section 2.2.2 but did not display any indication of a successful reaction. The Suzuki-Miyaura coupling of 4-nitroiodobenzene with phenylboronic acid was next tested, using K_2CO_3 as the base with a 3:1 ethanol/water solvent and 50°C matching the conditions of the planned one-pot synthesis. 13 of the palladium-loaded beads were used, and the reaction was left to run for 24 hours, where long needle crystals were formed in the vial. The product was extracted with ethyl acetate and 1 M $NaOH_{(aq)}$, and analysed by ^1H NMR spectroscopy, indicating no yield of the desired product.

At this point, the reason for the zero yield was identified as the low level of solubility of the 4-nitroiodobenzene in the 3:1 ethanol/water solvent, which was also seen as the same issue when testing its reduction with the silver-nanoparticle beads. We then attempted to identify conditions to facilitate the reaction to allow for the reagents to be solubilised while also forming a sufficient environment for the reagents to diffuse into the beads by having a solvent miscible with water.

4-Nitroiodobenzene is soluble in DCM, so we used 1:1 ethanol/DCM as the solvent, which provided a suitable level of solubility for all reagents while also maintaining a sufficiently hydrophilic environment for the hydrogel beads. On the first attempt of this with the new solvent, the base for the coupling, K_2CO_3, failed to dissolve in the much more organic environment, so we changed it to the organic base pyridine which readily dissolves in the organic environment. Additionally, prior to the reaction, the palladium-nanoparticle beads were submerged in ethanol in order to replace the water in the gel matrix. This was done in order to provide a stronger rate of diffusion into the beads by creating a more miscible barrier between the internal gel matrix and the external reaction system.

The reaction was ran for 24 hours at the lower temperature of 30°C to accommodate the low boiling point of DCM. Following the reaction period, the mixture was colourless with no solid present in the sample, which did mean that all reagents had successfully dissolved in the reaction mixture. The beads were removed with tweezers, the mixture was washed with water and 1 M $NaOH_{(aq)}$, and the organic layer was separated and concentrated under vacuum. ^1H NMR spectroscopy analysis indicated no formation of the 4-nitrobiphenyl product.

Despite this failure, we attempted the combined, one-pot, orthogonal synthesis involving the Suzuki-Miyaura coupling and nitro-reduction of 4-nitroiodobenzene. The reaction conditions would have to be adapted to support both reactions, particularly the nitro-reduction which had only been shown to work in aqueous conditions previously. We used 3:1 ethanol/water as the solvent, along with $NaBH_4$ to reduce the nitro-group, and phenylboronic acid and K_2CO_3 for the Suzuki-Miyaura coupling. The reaction time was kept at 24 hours which would give enough time for the Suzuki-Miyaura coupling to be finished (the nitro-reduction only required approximately three hours to be completed). The temperature was kept at 50°C, as the Suzuki-Miyaura coupling required higher temperatures for the reaction to occur.

We used 12 silver-nanoparticle and palladium-nanoparticle beads each, and added $NaBH_4$ last (as the mixture begins to effervesce strongly when it is added). Following the 24 hours, we found a turquoise blue precipitate in the vial, which when separated with ethyl acetate became a blue aqueous layer and a light green organic layer. The organic layer was concentrated and analysed by ^1H NMR spectroscopy, which did not show any noticeable signs of formation of the intended product (4-aminobiphenyl).

While solubility of the reagents had not been good in some of the reaction conditions over the series of experiments performed, it was theorised that it was the palladium-nanoparticle catalyst that had been the consistently failing factor in our reactions above all else, as even when the the conditions and beads had been adapted to the reagents (such as for the Suzuki-Miyaura coupling involving 1:1 DCM/ethanol), no product was formed. This was surprising based on previous studies from the group.[41] We therefore investigated the formation of the nanoparticles in the beads to identify the problem.

2.3.2. Change in Pd Nanoparticle Formation

Evidently the alginate beads loaded with palladium nanoparticles were not able to catalyse any reaction that was attempted, and further exploration was required to discover why they were not working. The first discrepancy noted was the colour of the beads; the palladium nanoparticles should give a dark brown colour as previously seen in Pd-nanoparticle loaded gels,[41] rather than the light orange that was observed on the beads. which indicated that Pd^{2+} had diffused into the beads but had not been reduced by the $DBS\text{-}CONHNH_2$. We used TEM to study the palladium beads on a more detailed level (Figure 2.2.3).

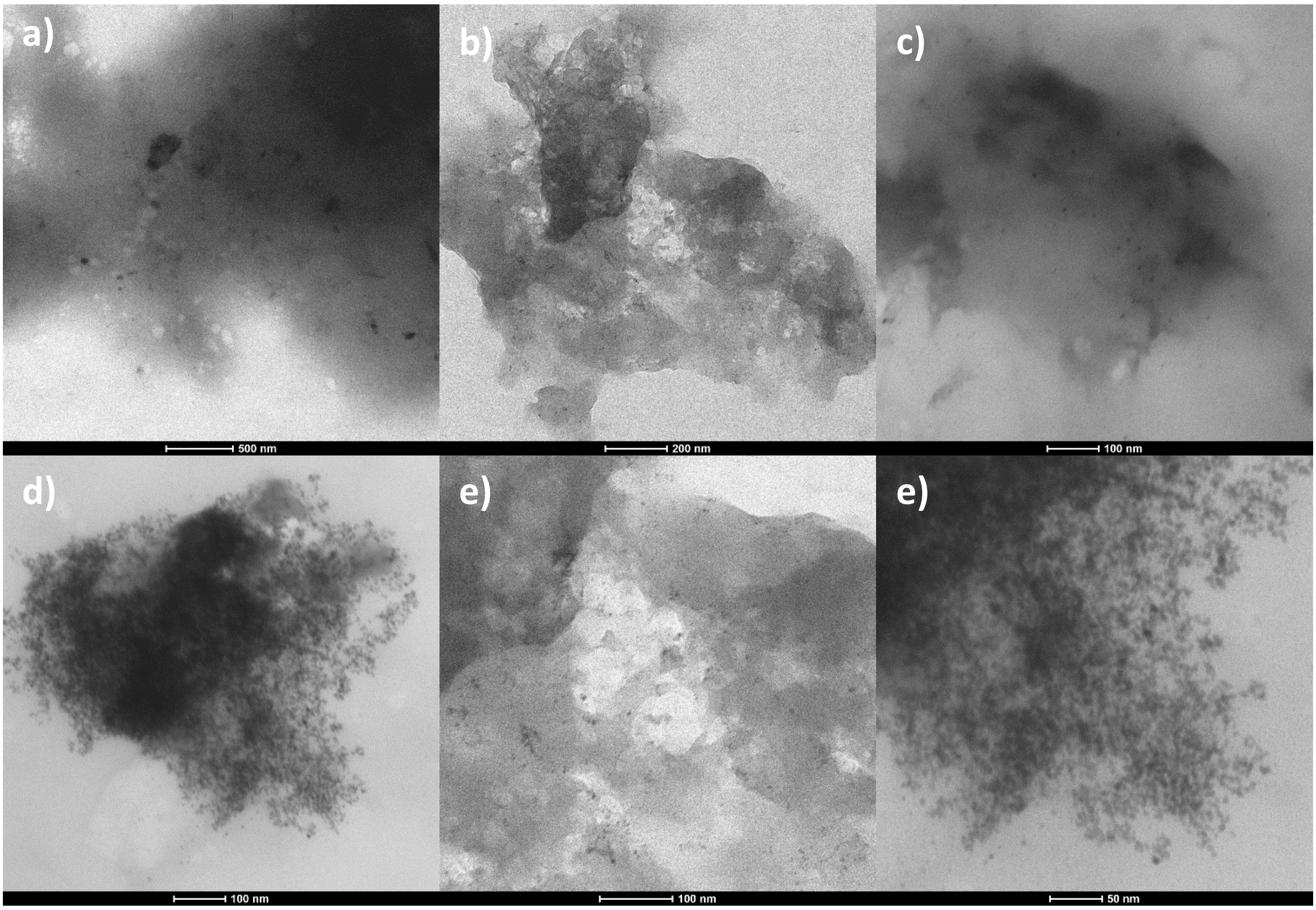

Figures 2.3.3 (a)-(f): TEM images of DBS-CONHNH$_2$/sodium alginate gel beads loaded with silver and palladium nanoparticles. Scale bars (a) 500 nm; (b) 200 nm; (c)-(e) 100 nm; (f) 50 nm

TEM revealed that there was very little development of nanoparticles in the gel matrix in this case, which meant there was not enough Pd(0) loaded to successfully catalyse any cross-couplings. The reason why the nanoparticles were not forming was found to be due to the low pH of the Pd^{2+} solution, which required HCl to dissolve the PdCl$_2$. While DBS-CONHNH$_2$ can form stable gels between pH 2-11.5, the high concentration of HCl gave a pH of 0.2-0.5 (measured by pH meter), which meant that the gels were not able to maintain their structure when added to the PdCl$_2$ solution. If the LMWG is destroyed in this way, then it cannot play the required active role of reducing the Pd^{II} to Pd^0 in situ, and hence nanoparticle will not form in the hybrid gel beads.

The Pd^{2+} solution was made less acidic to prevent dissolving the DBS-CONHNH$_2$, by first dissolving 50 mM PdCl$_2$ in a 0.1 M HCl solution, then diluting down to 5 mM Pd^{2+}. This in solution gave a pH of 2-3 and so the DBS-CONHNH$_2$ gel did not dissolve. After leaving the beads in the less acidic solution for three days, palladium nanoparticles had formed inside the beads, indicated by the darker brown colour when compared to the unreduced beads (Figure 2.3.4).

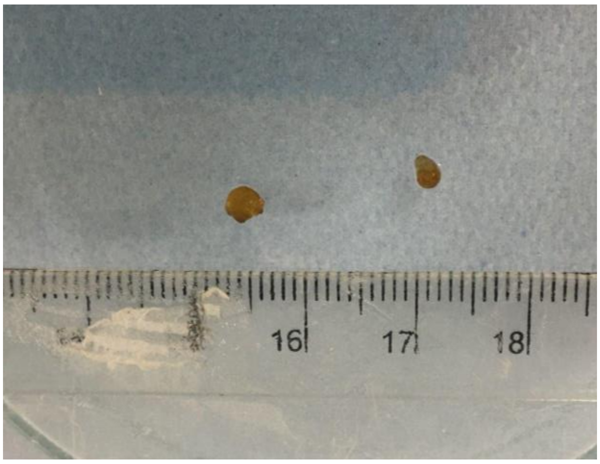

Figure 2.3.4 - DBS-CONHNH$_2$/Alginate Beads Loaded with Palladium Nanoparticles

The molar quantity of Pd^{2+} absorbed into the beads was measured via UV-Vis spectrometry. The peak for the Pd^{2+} solution was 425 nm, so a new calibration curve was needed to give the volume of Pd^{2+} taken in (Figure 2.3.5). For the DBS-CONHNH$_2$/alginate beads, uptake was found to be 0.0725 mmol per bead, and 0.072 mmol per DBS-CONHNH$_2$/agarose beads.

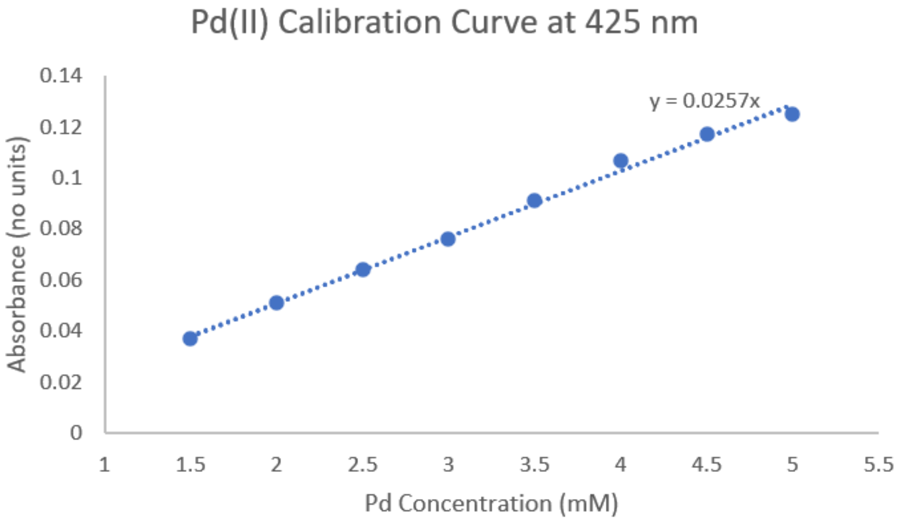

Figure 2.3.5 – Calibration curve of Pd(II)$_{(aq)}$ at 425 nm

New TEM images of the palladium nanoparticle DBS-CONHNH$_2$/alginate beads were taken to see if there was development of nanoparticles in the gel matrix (Figure 2.3.6).

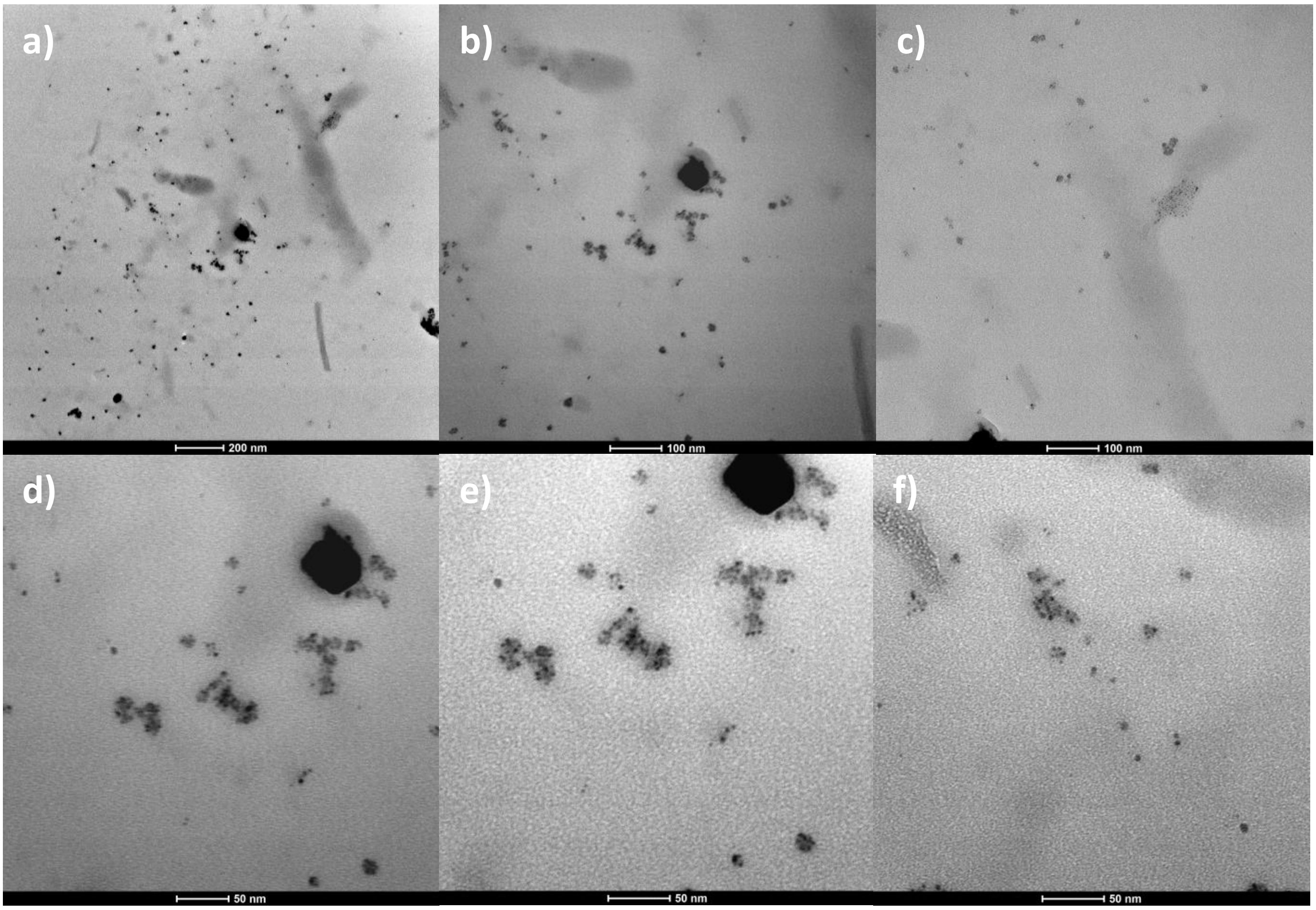

Figure 2.3.6 (a)-(f): TEM Images of DBS-CONHNH$_2$/alginate Loaded with Palladium Nanoparticles. Scale Bars (a) 200 nm; (b) and (c) 100 nm; (d) – (f) 50 nm

The TEM images demonstrated the formation of palladium nanoparticles in the DBS-CONHNH$_2$/alginate, as seen by the dark spots on the images. The new DBS-CONHNH$_2$/alginate beads were tested for their capability to catalyse the Suzuki-Miyaura cross-coupling, using 4-iodophenol and phenylboronic acid (Figure 2.2.6). 4-iodophenol was chosen as the coupling partner due to its greater hydrophilicity than common aromatic halides, such as bromobenzene or 4-nitroiodobenzene used in earlier experiments. Potassium Carbonate was used as the base, and the solvent 3:1 ethanol/water solution. The reaction system was left at 50 °C for 24 hours.

The resulting reaction mixture after 24 hours was clear, and the beads had turned black in colour. The solution was simply removed via pipette and the product was extracted with diethyl ether and washed with 1 M NaOH$_{(aq)}$ and water. The organic layer was concentrated and gave a white powder.

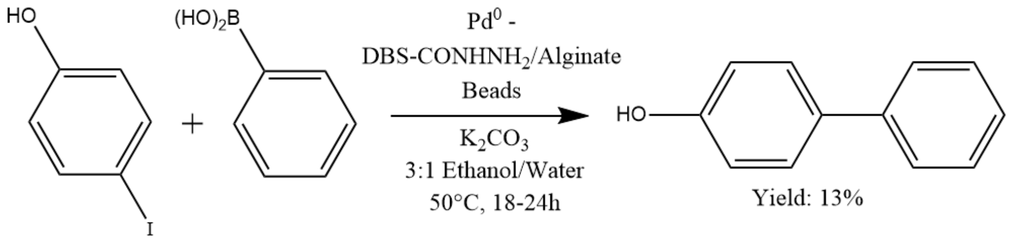

Figure 2.3.6: Suzuki-Miyaura coupling between 4-iodophenol and phenyl boronic acid

^{1}H NMR spectroscopy showed that 4-phenylphenol had been successfully synthesised, using the alginate beads loaded with palladium as the catalyst support. While the aromatic region of the ^{1}H NMR spectrum of 4-phenylphenol is difficult to interpret, a large singlet at approximately 4.95 ppm corresponding to the hydroxyl proton indicated its formation. Disappointingly, however, a yield of only 13% was achieved.

We then probed the ability of the agarose-based beads to produce palladium nanoparticles and perform the same cross-coupling as the DBS-CONHNH$_2$/agarose gel beads. Pd-NPs were grown in the same solution as the alginate-based beads for three days, after which we observed the development of nanoparticles in the gel matrix. This was first indicated by the change to the dark brown colour of the beads, similar to the colour of the DBS-CONHNH$_2$/alginate beads loaded with Pd-NPs (Figure 2.2.7).

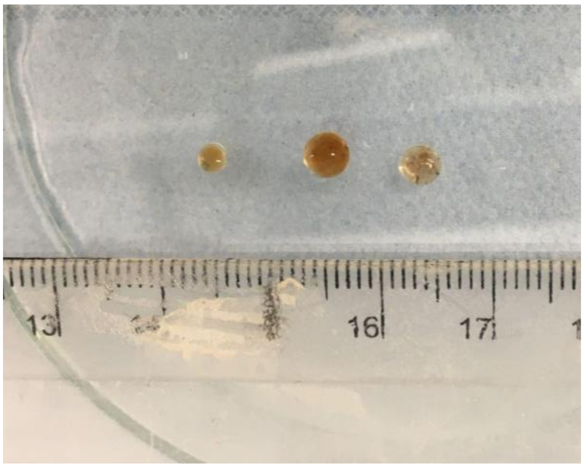

Figure 2.3.7 - DBS-CONHNH$_2$/Agarose Beads loaded with Palladium Nanoparticles

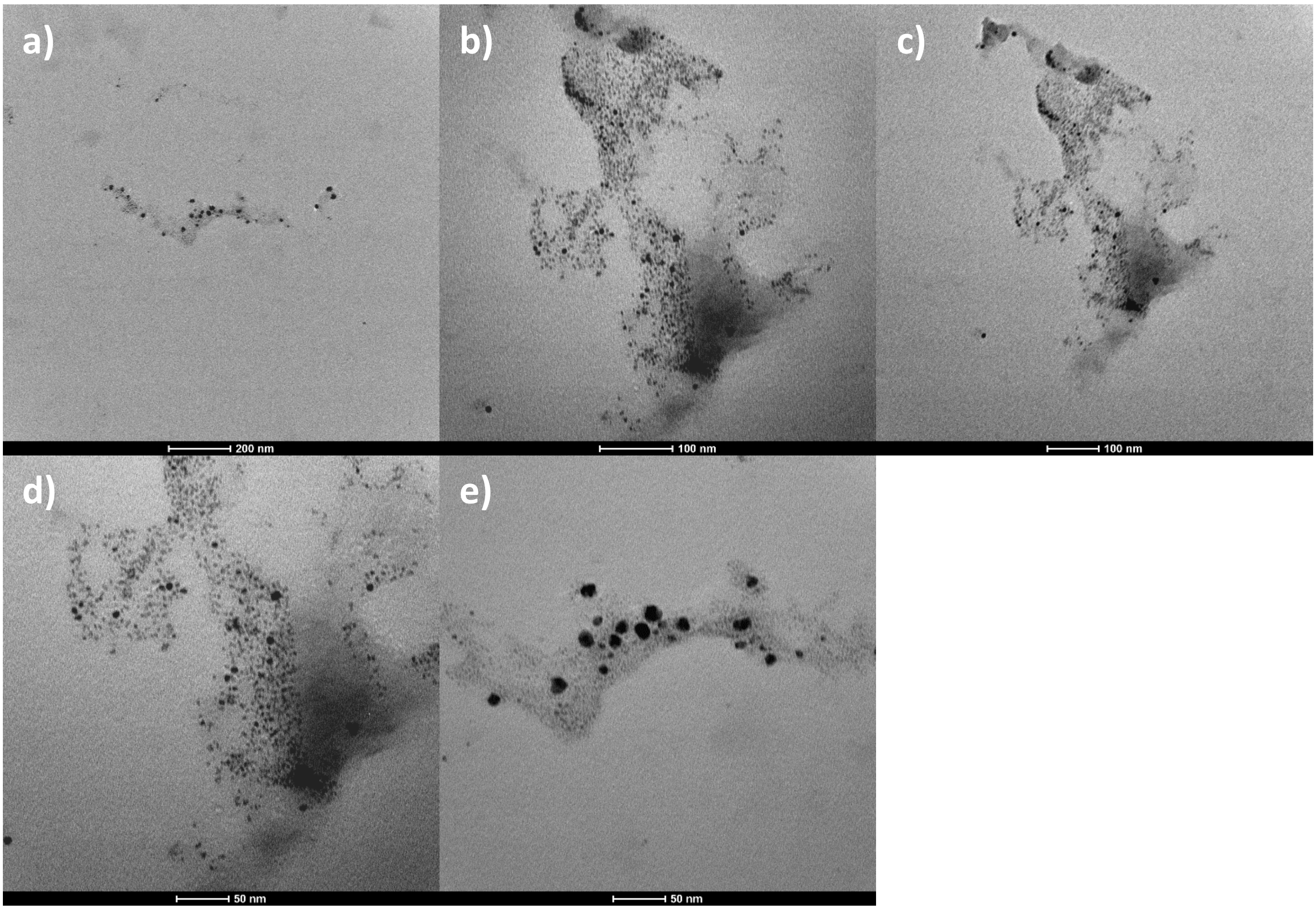

Figure 2.3.8: TEM Images of DBS-CONHNH$_2$/agarose gel beads loaded with Pd Nanoparticles. Scale bars (a) 200 nm; (b) and (c) 100 nm; (d) and (e) 50 nm

The agarose beads were further studied by TEM in Figure 2.3.8, which revealed that nanoparticles had formed tightly uniformly along the nanofibres with a spherical shape (Figure 2.2.8). The average diameter of the nanoparticles ranged between 1-10 nm, however some measured up to 35 nm, indicating some aggregation had occurred.

The DBS-CONHNH$_2$/agarose beads loaded with palladium were then used to catalyse the Suzuki-Miyaura cross-coupling of 4-iodophenol with phenylboronic acid, with potassium carbonate used as the base. After 24 hours of heating the reaction at 50 °C, the reaction product was extracted with diethyl ether and concentrated to a white solid. The product was analysed by ^{1}H NMR spectroscopy, and the alcohol singlet at 4.95 ppm indicated that 4-phenylphenol had been synthesised in a yield of 37%.

2.4. Multi-Nanoparticle

2.4.1. Development of Palladium and Silver Nanoparticles

As silver and palladium nanoparticles had been demonstrated to be successfully synthesised in both DBS-CONHNH$_2$/agarose and DBS-CONHNH$_2$/sodium alginate gel beads, we looked to combine both nanoparticles into one singular bead. We would therefore gain a multi-nanoparticle bead with the potential to carry out a variety of reactions, while the hydrogel support would allow for easy handling.

To produce the multi-nanoparticle beads, the two nanoparticle species had to be added consecutively. This is because Ag$^+$ in the presence of PdCl$_2$ solution will precipitate out into AgCl, so it would not be possible to add both at the same time. The Pd nanoparticles were grown first in the 5 mM PdCl$_2$ solution for three days, then the beads were washed in water over 2 days to allow the Cl$^-$ ions to diffuse out from the beads. The washed beads were then added to the 6.25 mM AgNO$_3$ solution to grow the silver nanoparticles, and were removed after three days. The beads were washed with water to remove superficial silver ions and stored in water for longer-term use.

After three days, both the alginate (Figure 2.2.9) and agarose (Figure 2.2.10) multiple-nanoparticle beads were much darker in colour than the single-nanoparticle beads, with a greyish matrix and darker, black spots throughout.

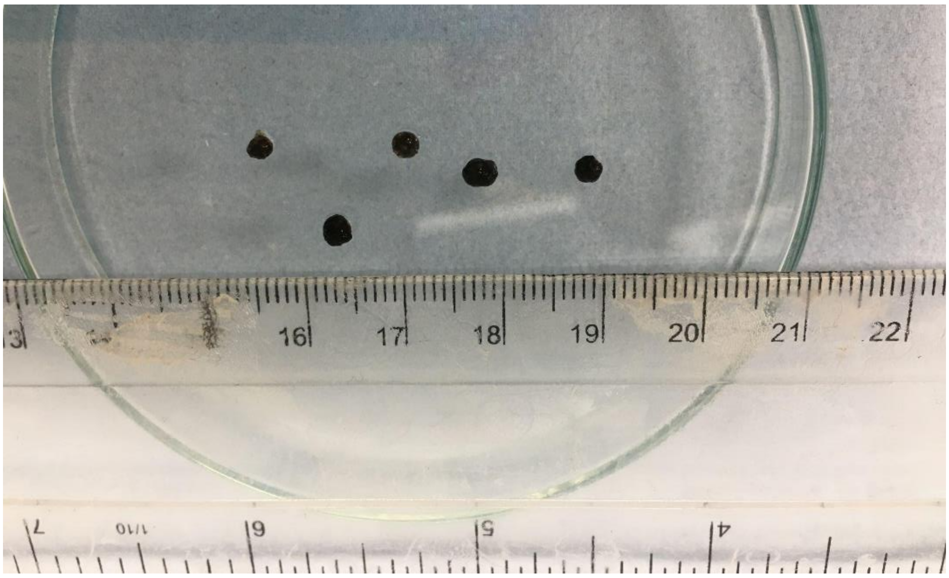

Figure 2.4.1 - DBS-CONHNH$_2$/sodium alginate hybrid hydrogel beads loaded with silver and palladium nanoparticles

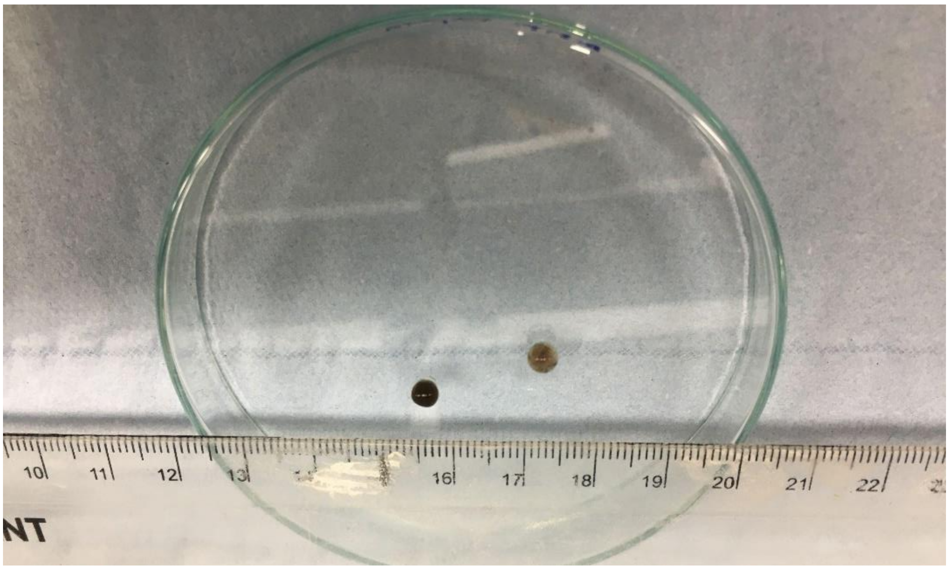

Figure 2.4.2: DBS-CONHNH$_2$/agarose hybrid hydrogel beads loaded with silver and palladium nanoparticles

The two bead species were further studied using TEM to study the distribution and size of the two different metal nanoparticles (Figure 2.4.3).

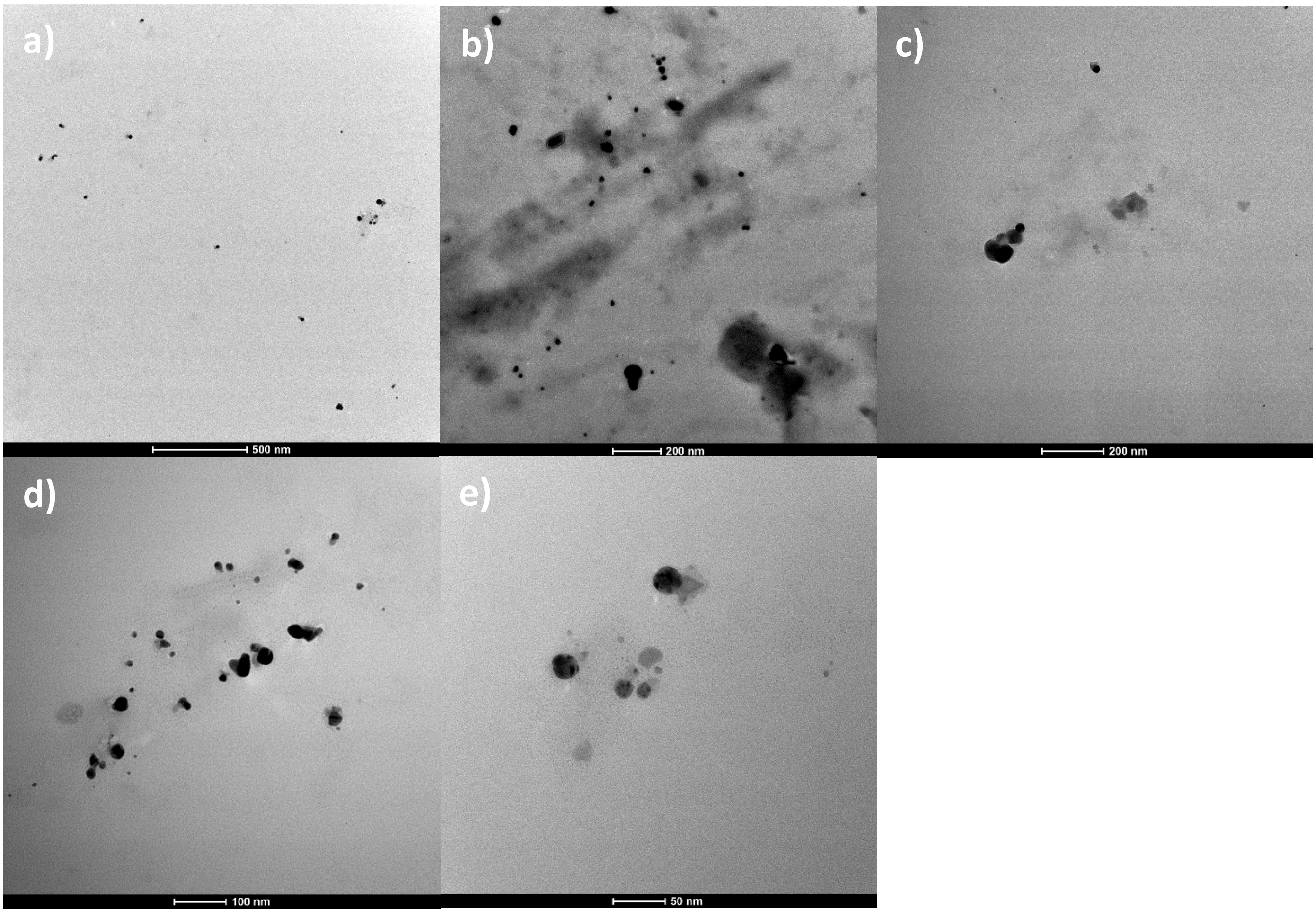

Figures 2.4.3 (a)-(e): TEM images of DBS-CONHNH$_2$/sodium alginate gel beads loaded with silver and palladium nanoparticles. Scale bars (a) 500 nm; (b) and (c) 200 nm; (d) 100 nm; (e) 50 nm

The DBS-CONHNH$_2$/sodium alginate gel beads produced nanoparticles with a round shape, but significant dispersity in size within the sample, with some larger nanoparticles measuring at 120 nm as seen in image (b)), whereas many are in the expected 1-10 nm range. The smaller nanoparticle sizes indicated that Ag(0) atoms were not aggregating on top of the palladium nanoparticles once they had been reduced, which would lead to a greater average size.

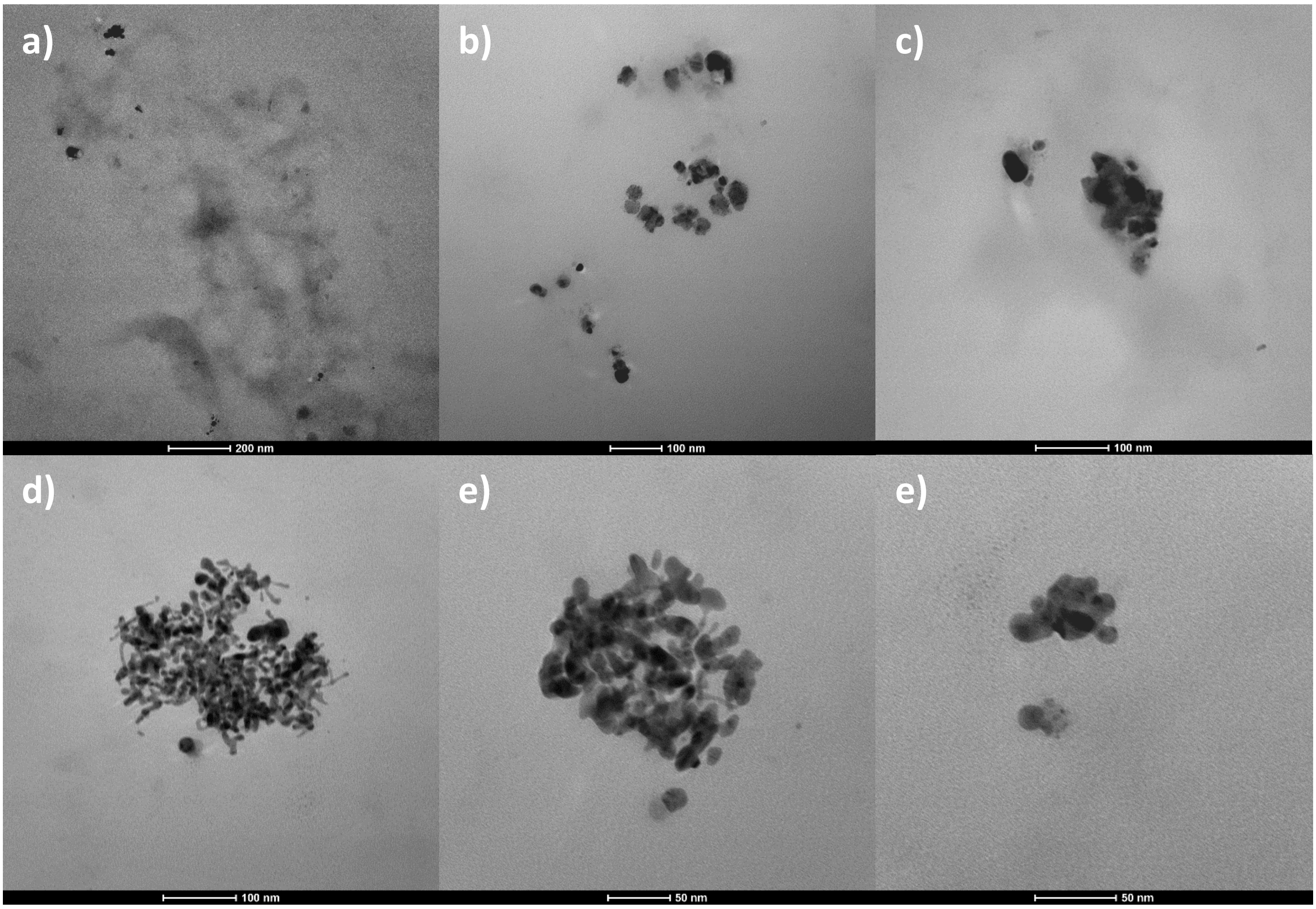

Figures 2.4.4 (a)-(f): TEM images of DBS-CONHNH$_2$/agarose gel beads loaded with silver and palladium nanoparticles. Scale bars (a) 200 nm; (b), (c) and (d) 100 nm; (e) and (f) 50 nm.

Conversely, the TEM of the DBS-CONHNH$_2$/agarose gel beads in Figure 2.4.4 suggested that the nanoparticles present had much larger disparity in size when compared with the sodium alginate beads, and that some aggregation had occurred between the nanoparticles, as images (d) and (e) demonstrate.

2.4.2. Catalytic Study

We then tested the catalytic ability of the multi-nanoparticle beads. We first tested the ability of the silver nanoparticles to reduce 4-nitrophenol to 4-aminophenol in the presence of $NaBH_4$. The same procedure that was used for the single-silver nanoparticle beads was used for the agarose-based multi-nanoparticle beads, with water as the solvent and a room temperature reaction.

After three hours the reaction mixture was clear, indicating a successful conversion to 4-aminophenol. The beads were removed with tweezers, then the product was extracted with ethyl acetate and washed with water and 1 M $NaOH_{(aq)}$. The organic layer was dried with $MgSO_4$ and concentrated, yielding a grey solid. The reaction gave a 43% yield, which was lower than the 4-NP reduction catalysed by silver-only beads (68%) (Figure 2.2.2). It is possible that loading the beads with Ag after they have been loaded with Pd means that the loading of silver nanoparticles is less than in the silver nanoparticle-only gel.

The multi-nanoparticle beads were then probed to catalyse the Suzuki-Miyaura cross-coupling, again between 4-iodophenol and phenylboronic acid using potassium carbonate as the base.

After 24 hours the solution was colourless, and the beads had darkened in colour. The beads were removed using tweezers, and the product was extracted with diethyl ether, washed with water and 1 M $NaOH_{(aq)}$, and the organic layer was dried with $MgSO_4$ and concentrated, giving a white powder. ^{1}H NMR spectroscopy and results taken indicated a 52% yield of 4-phenylphenol, meaning that the reaction had been more successful than the single nanoparticle gel beads.

The next step of exploration of the multi-nanoparticle hydrogel beads would be two orthogonal processes on a single molecule, similar to the attempted two-step reaction using separate silver and palladium beads. However, time did not allow for us to complete this stage of research.

3. CONCLUSION

DBS-CONHNH$_2$ was successfully synthesised as previously reported and was used to produce hybrid hydrogel beads with both sodium alginate and agarose. The DBS-CONHNH$_2$/alginate beads were 3 mm in diameter on average, whereas the DBS-CONHNH$_2$/agarose had a larger disparity in size, typically between 2.5-5 mm in diameter.

Silver nanoparticles were also successfully embedded into both species of hydrogel bead, via uptake of Ag^+ from the supernatant solution followed by *in situ* reduction, leading to aggregation of the atoms into nanoparticles. The hybrid hydrogel beads combined with sodium alginate were found to be taking in between 0.1-0.5 μmol per bead, meaning 10 gel beads gave approximately 1 mol% catalyst for the nitro-arene reductions. Similarly, the DBS-CONHNH$_2$/agarose gel beads uptake of silver was on average between 0.1-0.3 μmol in the samples tested.

We found that the silver nanoparticles were capable of catalysing the reduction of a number of nitro-arenes to their respective anilines in the presence of sodium borohydride. 4-nitrophenol and 2-nitrophenol were successfully reduced to 4-aminophenol and 2-aminophenol respectively in 68 and 69% yields, without the need for higher temperatures, long reaction times and toxic chemicals. The isomer 3-nitrophenol however was not able to be reduced successfully. Both hydrogel bead species were able to be effectively recycled for multiple reductions of 4-nitrophenol, however mechanical degradation meant the number of recycles was limited to two.

The DBS-CONHNH$_2$ hybrid hydrogel beads combined with agarose and alginate have been demonstrated *in situ* development of silver nanoparticles and provide a simple method of catalysis that can produce high yields of product. Furthermore, they are also an environmentally friendly method of recycling precious metal catalysts.

After successfully embedding palladium nanoparticles in hydrogel beads as well as catalysing the Suzuki-Miyaura cross-coupling between 4-iodophenol and phenylboronic acid, both silver and palladium nanoparticles were added to the same gel matrix. Both nanoparticles were successfully grown within the gels, and used to catalyse both a 4-nitrophenol reduction using the silver nanoparticles (43% yield), and a Suzuki-Miyaura cross-coupling using the palladium nanoparticles (52% yield).

In the multi-nanoparticle gel beads, we have therefore developed a highly versatile tool that can catalyse an array of reactions. In addition to this, the gel beads are safe to handle and easy to add and remove from reaction systems, removing the need for a potentially time-consuming and difficult work-up.

4. FUTURE WORK

As the DBS-CONHNH$_2$ hydrogel supports have been demonstrated to support multiple nanoparticles that can be used for catalysis, this can be expanded to orthogonal processes on a single species. For example, a nitro-aromatic-halide can potentially have its nitro-group reduced to an amine because of the presence of silver nanoparticles, and can also be coupled with boronic acids in a palladium catalysed Suzuki-Miyaura cross-coupling. This would provide a versatile tool for catalyst delivery that could be easily used and removed from a system and could further be recycled for multiple reactions.

As the recyclability of silver-nanoparticle gel beads was notably poor for the reduction of 4-nitrophenol, the polymer gelator could be replaced with a different gelator for improved performance. Examples such as the synthetic polymer gelator *N*,*N*,-dimethylacrylamide[54] can be combined with DBS-CONHNH$_2$ to provide greater resistance to sodium borohydride.

5. EXPERIMENTAL

5.1. General Methods and Materials

All reagents were supplied from commercial sources and used without additional purification unless stated otherwise.

^{1}H and ^{13}C NMR was performed via JEOL ECX400 (400 MHz 1H NMR, 100 MHz 13C NMR)

UV-Vis absorbance was measured using Shimadzu UV-2401PC spectrophotometer

Transmission Electron Microscopy was performed with the help of Karen Hodgkinson of the Bioscience Technology Facility, Department of Biology, University of York, using an FEI Tecnai 12 G^2 fitted with a CCD camera

Mass Spectrometry, EI and ESI, was performed with the help of Karl Heaton using a Bruker Daltonics MicroTOF mass spectrometer

5.2. Formation of Hybrid Hydrogel Beads and Metal Nanoparticle Loading

5.2.1. Alginate Beads Formation

Method

0.25 g of sodium alginate was added to 25 ml of water, and mixed for a minimum of 90 minutes, until the sodium alginate was completely dissolved to give a 1% wt/vol solution .

Initially 0.3% wt/vol (3 mg) of DBS-CONHNH$_2$ was added to a 2 ml vial, then 0.75 ml of 1% wt/vol sodium alginate and 0.25 ml of water. The mixture was sonicated at room temperature for 15 minutes, which yielded a cloudy white mixture. The vial was heated until complete dissolution, following which the cap was slowly removed to prevent bumping, then allowed cooling for around 60 seconds until it gelated enough to invert. Once inversion is possible, the gel was added dropwise in 50 µl aliquots (16.7 µl/drop) to approximately 40 ml of 5% wt/vol CaCl$_2$ solution. The beads were obtained by filtration and washed with water.

5.2.2. Agarose Beads Formation

Method

0.3% wt/vol (3 mg) DBS-CONHNH$_2$ and 1.0% wt/vol (10 mg) agarose was added to 1.0 ml of water in a 2 ml vial and sonicated for 15 minutes. The suspension was then heated until complete dissolution, and added in 50 µl aliquots dropwise into cold paraffin oil. The beads were left for 20 minutes to allow for full gelation of the two networks in the oil. To remove the residual paraffin oil, the beads were isolated and washed in petroleum ether (30 ml, 30 minutes), ethanol (30 ml, 30 minutes) then water (30 ml, 30 minutes) before finally being stored long-term in water.

5.2.3. Palladium Nanoparticle Loading

Method

264.48 mg PdCl$_2$ was dissolved in 30 ml of 0.1 M HCl, using sonication to promote complete solvation. The 50 mM Pd^{2+} solution was diluted by 10x in water to give a 5 mM Pd^{2+} in 0.01 M HCl. Hybrid hydrogel beads were immersed in 3 ml of 5 mM Pd^{2+} and left for 72 hours to allow time for nanoparticles to form. After 3 days, beads were removed from the supernatant, washed with water to remove superficial Pd^{2+} and left in water for long term storage.

Pd^{2+} uptake was measured by calculating the change in supernatant concentration using UV-Vis spectroscopy.

5.2.4. Silver Nanoparticle Loading

Method

Hybrid hydrogel beads were immersed in 3 ml of 6.25 mM Ag^+ and the vial was covered with tin foil to protect the sample from light. After three days, the beads were removed, washed with water to remove superficial Ag^+ and left in water for long term storage.

Ag^+ uptake was measured by titrating with 0.05 mM NaCl and 2.5% K_2CO_3 to determine the remaining Ag^+ concentration in the supernatant.

5.3. Synthesis of Compounds

5.3.1. DBS-CO_2Me Synthesis

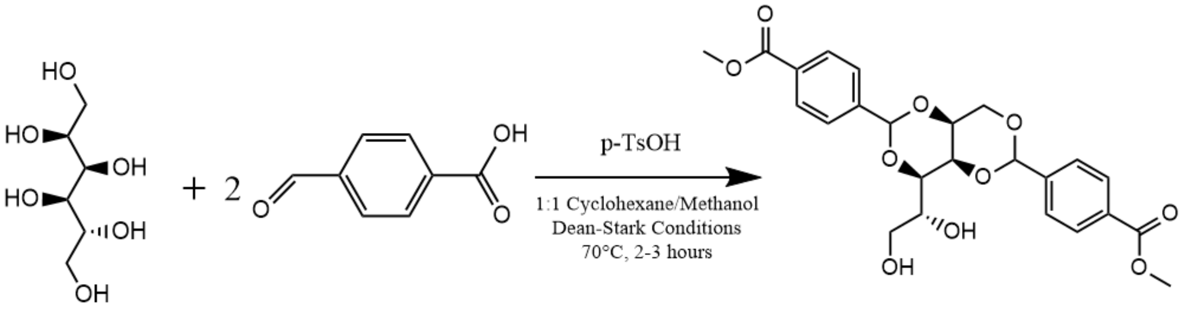

D-sorbitol (5.10 g, 27.0 mmol) was added to a solution of cyclohexane (70 ml) and methanol (30 ml) under nitrogen and stirred at room temperature for 20 minutes. After stirring, 4-methylcarboxybenzaldehyde (7.50 g, 49.9 mmol) and p-toluenesulfonic acid monohydrate (1.00 g, 5.59 mmol) dissolved in 40 ml of methanol was added to the reaction mixture, and the system was heated for 2-3 hours, adding additional solvent after 1 hour (7:3 cyclohexane/methanol). After most of the solvent had been removed from the mixture, the resulting white solid was dried over vacuum, washed with methanol and left to air dry overnight. The solid was then washed by refluxing in water (3 x 100 ml) for 30 minutes, then refluxing in DCM (3 x 100 ml) for 30 minutes. The residual solid was left to dry over the vacuum to remove DCM.

Yield: 3.49 g (26.3%)

NMR: ^1H NMR (400 MHz, DMSO-D6) δ 7.96-7.93 (m, 4H, ArH_1), 7.59-7.54 (m, 4H, ArH_2) 5.72 (s, 2H, Ar-CH_1) 4.90 (d, 1H, $CHOH$, J=8) 4.44 (t, 1H, CH_2OH, J=4) 4.18-4.16 (m, 3H, $H_{3,4,5}$), 3.97 (s, 1H, C*H*O), 3.81(s, 6H, CO_2CH_3), 3.60-3.55 (m, 1H, C*H*O) 3.47-3.40 (m, 1H, C*H*O)

5.3.2. DBS-CONHNH$_2$ Synthesis

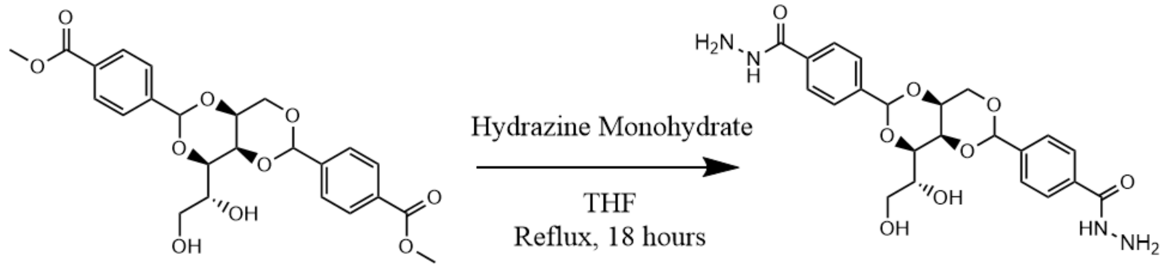

DBS-CO$_2$Me (1.10 g, 2.32 mmol) was dissolved in THF (70 ml). Hydrazine monohydrate (6 ml, 123.7 mmol) was added *via* syringe, and the reaction was left to heat overnight at reflux. After cooling to room temperature, the resulting white solid was washed with water (6 x 50 ml), then dried first under high vacuum, then in a vacuum oven until it had reached a constant mass.

Yield: 0.99 g (89.5 %)

NMR: ^{1}H NMR (400 MHz, DMSO-D6) δ 9.76 (s, 2H, CO$_2$N*H*NH$_2$), 7.80-7.77 (m, 4H, Ar*H*), 7.50-7.45 (m, 4H, Ar*H*) 5.67 (s, 2H, ArC*H*) 4.88 (d, 1H, CHO*H, J=8*) 4.45-4.40 (m, 4H, NHN*H*$_2$) 4.16-4.14 (m, 3H, OCH$_{3,4,5}$) 3.94 (s, 1H, CHO) 3.84-3.81 (m, 1H, CHO) 3.73 (m, 1H, CHO), 3.58-3.55 (m, 1H, CHO),

5.3.3. 4-Nitrophenol Reduction

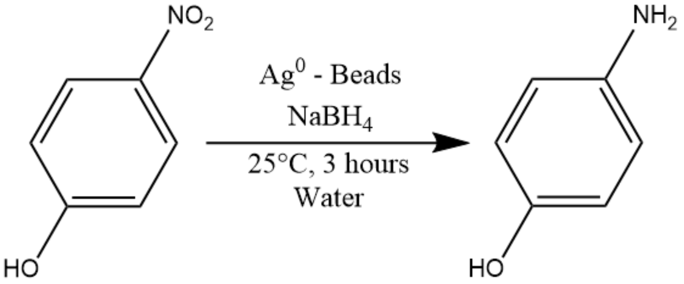

DBS-CONHNH$_2$/sodium alginate hybrid hydrogel beads loaded with silver nanoparticles were added to 5 ml of water in a 7ml vial, followed by 4-nitrophenol (30 mg, 0.216 mmol) and sodium borohydride (81.6 mg, 0.216 mmol), after which the vial was sealed with the cap and left at room temperature. After 45 minutes, the vial was briefly opened to allow the release of hydrogen gas, the sealed after. After 3 hours, the gel beads were removed from the mixture, the product was extracted with ethyl acetate and concentrated over vacuum.

Yield: 26.07 mg (68%)

^{1}H NMR (300 MHz, DMSO) δ 8.33 (s, 1H, ArO*H*) 6.50, 6.49, 6.49-6.40 (m, 4H, Ar*H*) 4.36 (s, 2H, NH$_2$)

5.3.4. 2-Nitrophenol Reduction

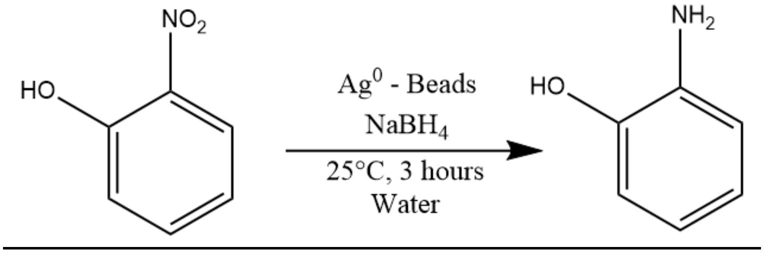

DBS-CONHNH$_2$/sodium alginate hybrid hydrogel beads loaded with silver nanoparticles were added to 5 ml of water in a 7ml vial, followed by 2-nitrophenol (30 mg, 0.216 mmol) and sodium borohydride (81.6 mg, 0.216 mmol), after which the vial was sealed with the cap and left at room temperature. After 45 minutes, the vial was briefly opened to allow the release of hydrogen gas, the sealed after. After 3 hours, the gel beads were removed, and the product was extracted with ethyl acetate. The organic layer was washed with 1 M NaOH$_{(aq)}$ and concentrated over vacuum.

Yield: 16.2 mg (69%)

^{1}H NMR (400 MHz, DMSO-d$_6$): δ 8.89 (s, 1H, OH), 6.60-6.49 (m, 3H, ArH), 6.36-6.32 (t, 1H ArH, J=8Hz), 4.43 (s, 2H, NH)

5.3.5. 3-Nitrophenol Reduction

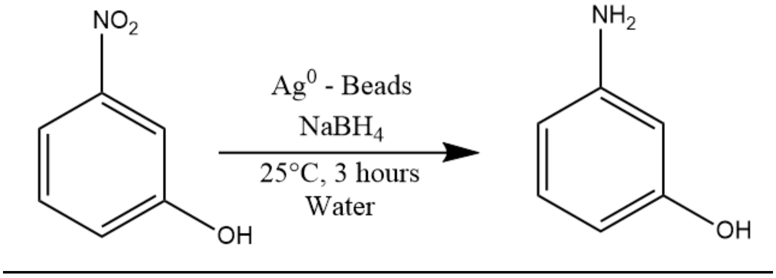

DBS-CONHNH$_2$/sodium alginate hybrid hydrogel beads loaded with silver nanoparticles were added to 5 ml of water in a 7ml vial, followed by 3-nitrophenol (30 mg, 0.216 mmol) and sodium borohydride (81.6 mg, 0.216 mmol), after which the vial was sealed with the cap and left at room temperature. After 45 minutes, the vial was briefly opened to allow the release of hydrogen gas, the sealed after. After 3 hours, the gel beads were removed, and the product was extracted with diethyl ether. The organic layer was washed with 1 M NaOH$_{(aq)}$ and concentrated over vacuum.

Yield: 0%

5.3.6. 4-Nitroiodobenzene Reduction

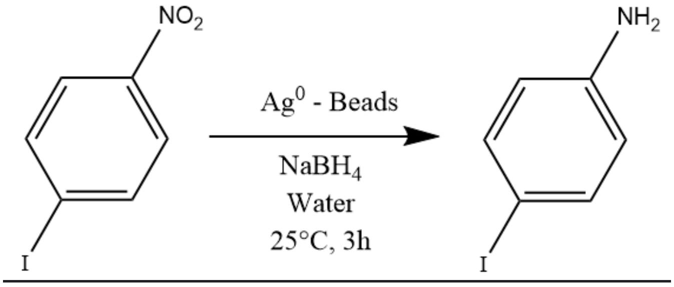

Gel beads loaded with silver nanoparticles were added to 5 ml of water in a 7ml vial, followed by 4-nitroiodobenzene (114.54 mg, 0.46 mmol) and sodium borohydride (35.94 mg, 0.95 mmol), after which the vial was sealed with the cap and left at 50 °C. After 45 minutes, the vial was briefly opened to allow the release of hydrogen gas, the sealed after. After 24 hours, the gel beads were removed from the mixture and the product was extracted with diethyl ether and 1 M $NaOH_{(aq)"}$".

Yield: 0% (Returned starting material)

5.3.7. 2-Nitrobenzyl Alcohol Reduction

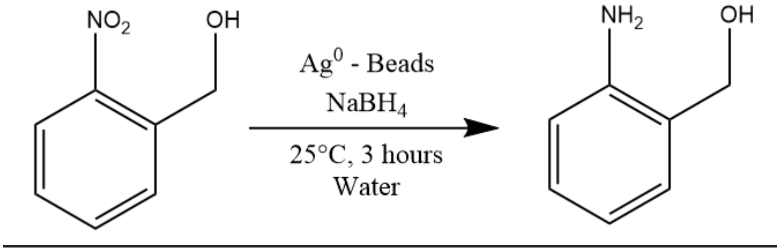

DBS-$CONHNH_2$/sodium alginate hybrid hydrogel beads loaded with silver nanoparticles were added to 5 ml of water in a 7ml vial, followed by 2-nitrobenzyl alcohol (33.08 mg, 0.216 mmol) and sodium borohydride (81.6 mg, 0.216 mmol), after which the vial was sealed with the cap and left at room temperature. After 45 minutes, the vial was briefly opened to allow the release of hydrogen gas, the sealed after. After 3 hours and 15 minutes, the gel beads were removed, and the product was extracted with diethyl ether and concentrated over vacuum.

Yield: 0%

5.3.8. 2-Nitrobenzaldehyde Reduction

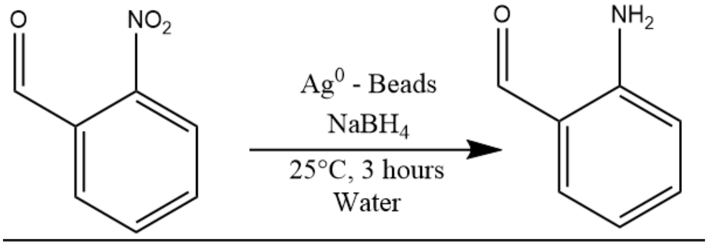

DBS-CONHNH$_2$/sodium alginate hybrid hydrogel beads loaded with silver nanoparticles were added to 5 ml of water in a 7ml vial, followed by 2-nitrobenzaldehyde (32.64 mg, 0.216 mmol) and sodium borohydride (81.6 mg, 0.216 mmol), after which the vial was sealed with the cap and left at room temperature. After 3 hours, the gel beads were removed by filtration on paper, and the mixture was washed with diethyl ether and concentrated over vacuum.

Yield: 0%

5.3.9. 3-Nitropyridine Reduction

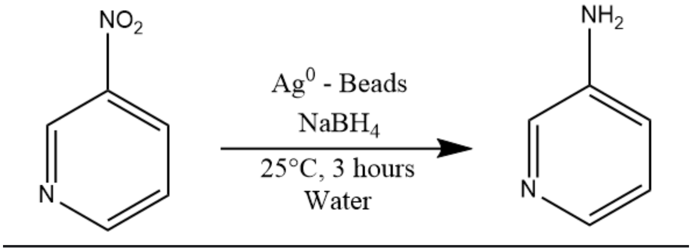

DBS-CONHNH$_2$/sodium alginate hybrid hydrogel beads loaded with silver nanoparticles were added to 5 ml of water in a 7ml vial, followed by 3-nitropyridine (26.81 mg, 0.216 mmol) and sodium borohydride (81.6 mg, 0.216 mmol), after which the vial was sealed with the cap and left at room temperature. After 3 hours, the gel beads were removed via filtering through paper, and the product was extracted with diethyl ether. The organic layer was washed with 1 M $NaOH_{(aq)}$ and concentrated over vacuum.

Yield: 0%

5.3.10. 2-Nitrobiphenyl Reduction

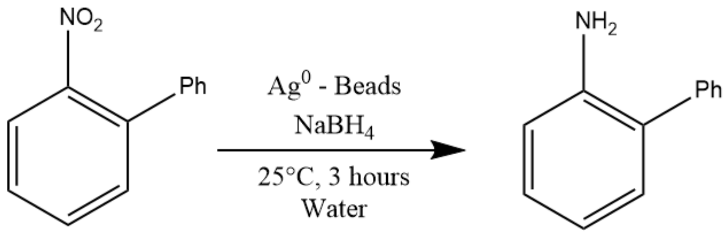

DBS-CONHNH$_2$/sodium alginate hybrid hydrogel beads loaded with silver nanoparticles were added to 5 ml of water in a 7ml vial, followed by 3-nitropyridine (43.03 mg, 0.216 mmol) and sodium borohydride (81.6 mg, 0.216 mmol), after which the vial was sealed with the cap and left at room temperature. After 3 hours, the gel beads were removed via filtering through paper, and the product was extracted with DCM. The organic layer was concentrated over vacuum.

Yield: 0%

5.3.11. 4-Nitrobiphenyl Reduction

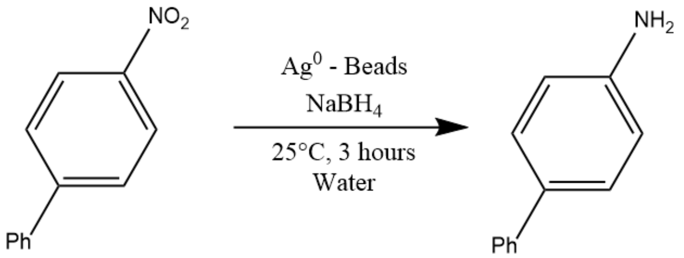

DBS-CONHNH$_2$/sodium alginate hybrid hydrogel beads loaded with silver nanoparticles were added to 5 ml of water in a 7ml vial, followed by 4-nitrobiphenyl (43.03 mg, 0.216 mmol) and sodium borohydride (81.6 mg, 0.216 mmol), after which the vial was sealed with the cap and left at room temperature. After 4 hours, the gel beads were removed via spatula, and the product was extracted with diethyl ether, washed with 1 M NaOH$_{(aq)}$, and concentrated over vacuum.

Yield: 0%

5.3.12. 4-(trifluoromethyl) nitrobenzene Reduction

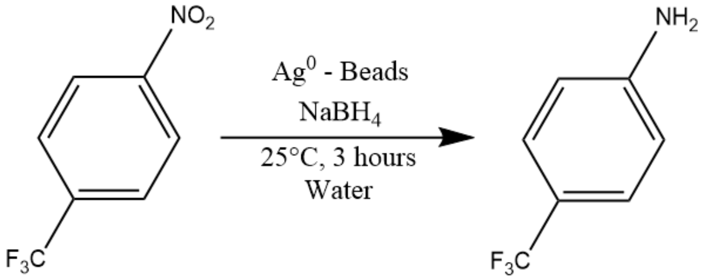

DBS-CONHNH$_2$/sodium alginate hybrid hydrogel beads loaded with silver nanoparticles were added to 5 ml of water in a 7ml vial, followed by 4-(trifluoromethyl) nitrobenzene (41.28 mg, 0.216 mmol) and sodium borohydride (81.6 mg, 0.216 mmol), after which the vial was sealed with the cap and left at room temperature. After 3 hours, gel beads were removed by filtering through paper, and the product was extracted with diethyl ether, and concentrated over vacuum.

Yield: 0%

5.3.13. 1,3-Dinitrobenzene Reduction

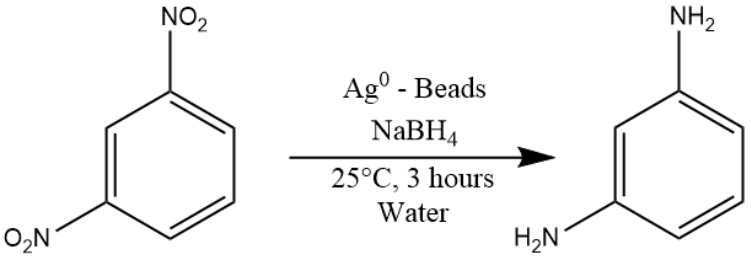

DBS-CONHNH$_2$/sodium alginate hybrid hydrogel beads loaded with silver nanoparticles were added to 5 ml of water in a 7ml vial, followed by 1,3-dinitrobenzene (36.31 mg, 0.216 mmol) and sodium borohydride (81.6 mg, 0.216 mmol), after which the vial was sealed with the cap and left at room temperature. After 3 hours, the gel beads were removed via filtering through paper, and the product was extracted with DCM. The organic layer was concentrated over vacuum.

Yield: 0%

5.3.14. Suzuki-Miyaura Cross-Coupling

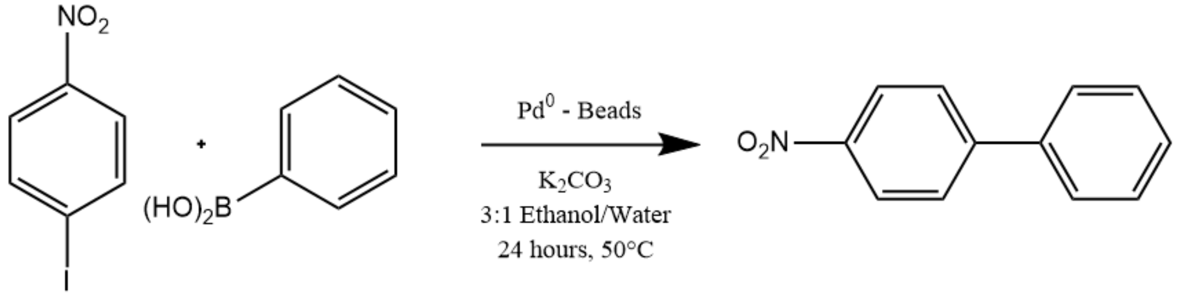

Gel beads loaded with palladium nanoparticles were added to a 7 ml vial with 5 ml of 3:1 ethanol/water. 4-nitroiodobenzene (0.46 mmol, 114.54 mg), phenyl boronic acid (0.58 mmol, 70.72 mg) and K_2CO_3 (0.97 mmol, 137.46 mg) were added to the vial, which was then sealed and heated at 50 °C. After 24 hours, the vial was taken off the heat and allowed to cool to room temperature. The product was extracted with diethyl ether and 1 M $NaOH_{(aq)}$, and the solvent was evaporated under reduced pressure.

Yield: 0%

5.3.15. Suzuki-Miyaura Cross-Coupling and Nitro Reduction of 4-Nitroiodobenzene Reduction: One Pot Synthesis

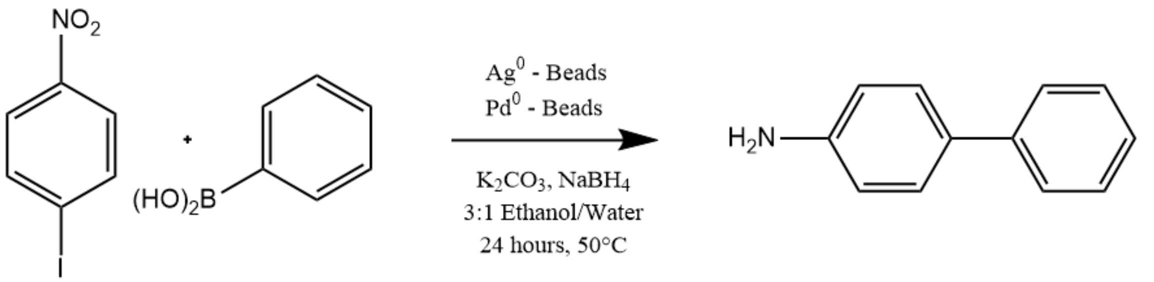

4-nitroiodobenzene (115.23 mg, 0.46 mmol), phenyl boronic acid (70.45 mg, 0.58 mmol) and potassium carbonate (132.00 mg, 0.96 mmol) were added to a 7 ml vial with Pd^0 and Ag^0 nanoparticle loaded beads in 5 ml of 3:1 ethanol/water solution. Sodium borohydride (77.29 mg, 2.04 mmol) was added last, and after addition the vial was quickly closed. The vial was heated at 50 °C for 24 hours, after which the product was extracted with diethyl ether and 1 M $NaOH_{(aq)}$. The organic layer was further washed with 1 M $NaOH_{(aq)}$, and the solvent was evaporated under reduced pressure.

Yield: 0% (returned 4-nitroiodobenzene)

5.3.16. 4-Iodophenol Suzuki-Miyaura Cross-Coupling with Phenylboronic Acid

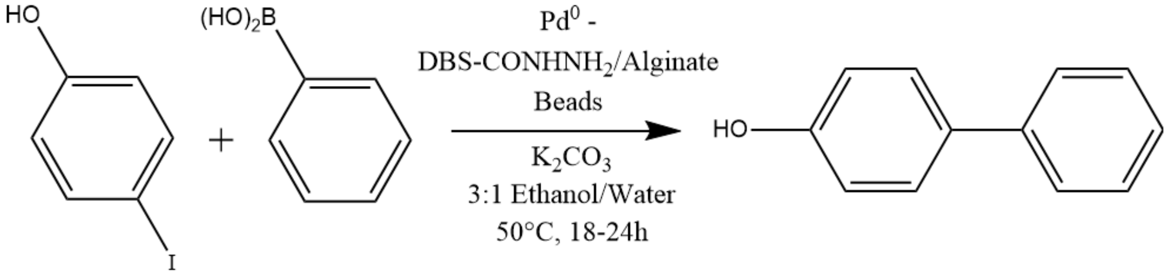

4-iodophenol (101.20 mg, 0.46 mmol), phenylboronic acid (70.72 mg, 0.58 mmol) and K_2CO_3 (134.06 mg, 0.97 mmol) were added to 5 ml 3:1 ethanol/water with $DBS-CONHNH_2$/sodium alginate beads loaded with palladium nanoparticles. The vial was heated at 50 °C for 24 hours, after which the beads were removed. The product was extracted with diethyl ether and washed with 1 M $NaOH_{(aq)}$ and water. The organic layer was concentrated under reduced pressure.

Yield: 10.13 mg (13 %)

^1H NMR (400 MHz, $CDCl_3$): δ 7.54 (dd, 2H, ArH, *J* = 8), 7.48 (dt, 2H, ArH, *J* = 8) 7.41 (t, 2H, ArH, J = 8) 7.31 (t, 1H, ArH, *J* = 8) 6.90 (d, 2H, ArH, J=8), 4.87 (s, 1H, OH)

5.3.17. 4-Iodophenol Suzuki-Miyaura Cross-Coupling with Phenylboronic Acid

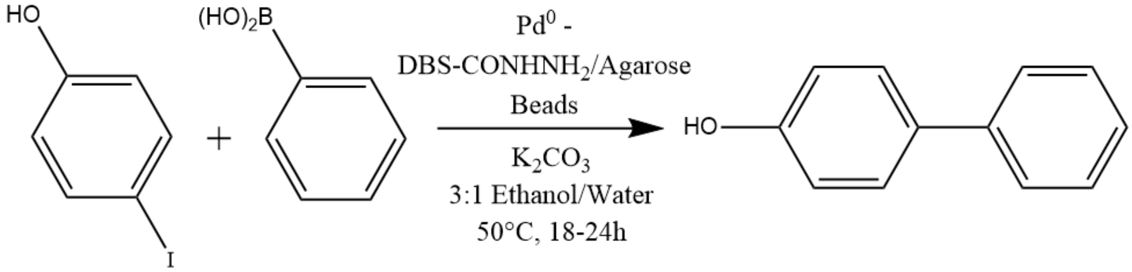

4-iodophenol (101.20 mg, 0.46 mmol), phenylboronic acid (70.72 mg, 0.58 mmol) and K_2CO_3 (134.06 mg, 0.97 mmol) were added to 5 ml 3:1 ethanol/water with $DBS-CONHNH_2$/agarose beads loaded with palladium nanoparticles. The vial was heated at 50 °C for 24 hours, after which the beads were removed. The product was extracted with diethyl ether and washed with 1 M $NaOH_{(aq)}$ and water. The organic layer was concentrated.

Yield: 29.06 mg (37 %)

^1H NMR (400 MHz, $CDCl_3$): δ 7.54 (dd, 2H, ArH, *J* = 8) 7.48 (dt, 2H, ArH, *J* = 8) 7.41 (t, 2H, ArH, *J* = 8) 7.31 (t, 1H, ArH, J = 8) 6.90 (d, 2H, ArH, *J* = 8), 4.87 (s, 1H, OH)

5.3.18. 4-Nitrophenol Reduction - Ag/Pd Agarose Beads

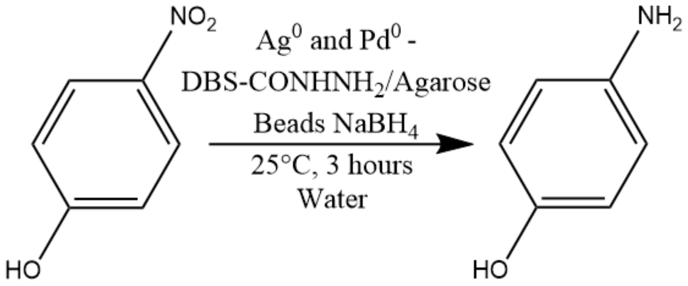

DBS-CONHNH$_2$/sodium alginate hybrid hydrogel beads loaded with silver nanoparticles were added to 5 ml of water in a 7ml vial, followed by 4-nitrophenol (30 mg, 0.216 mmol) and sodium borohydride (81.6 mg, 0.216 mmol), after which the vial was sealed with the cap and left at room temperature. After 45 minutes, the vial was briefly opened to allow the release of hydrogen gas, the sealed after. After 3 hours, the gel beads were removed from the mixture and the product was extracted with ethyl acetate. The organic layer was dried with $MgSO_4$ and concentrated over vacuum.

Yield: 10.2 mg (43%)

^{1}H NMR (400 MHz, DMSO-d$_6$): δ 8.31 (s, 1H, OH), 6.44-6.36 (m, 4H, ArH), 4.31 (s, 2H, NH)

5.3.19. 4-Iodophenol Suzuki-Miyaura Cross-Coupling with Phenylboronic Acid - Ag/Pd Agarose Beads

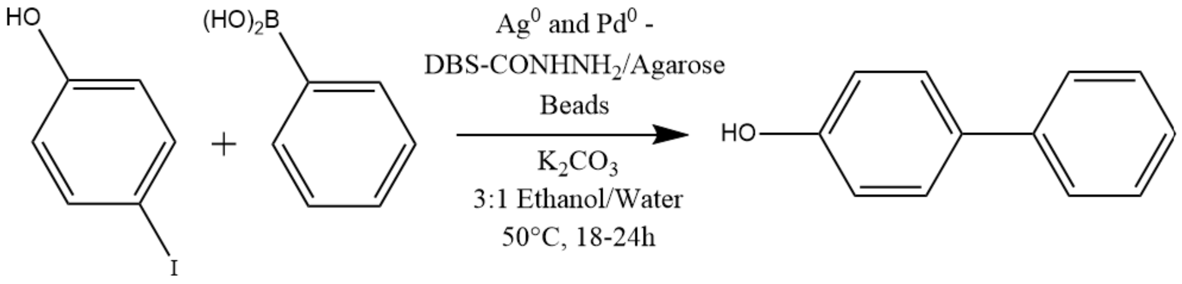

4-iodophenol (101.20 mg, 0.46 mmol), phenylboronic acid (70.72 mg, 0.58 mmol) and K_2CO_3 (134.06 mg, 0.97 mmol) were added to 5 ml 3:1 ethanol/water with DBS-CONHNH$_2$/agarose beads loaded with palladium and silver nanoparticles. The vial was heated at 50 °C for 24 hours, after which the beads were removed. The product was extracted with diethyl ether and washed with 1 M $NaOH_{(aq)}$ and water. The organic layer was concentrated under reduced pressure.

Yield: 40.6 mg (52 %)

^{1}H NMR (400 MHz, $CDCl_3$): δ 7.53 (dd, 2H, ArH, J = 8), 7.47 (dt, 2H, ArH, J = 12), 7.41 (t, 2H, ArH, J = 8) 7.30 (t, 1H, ArH, J = 12) 6.90 (d, 2H, ArH, J = 8), 4.97 (s, 1H, OH)

6. Appendix

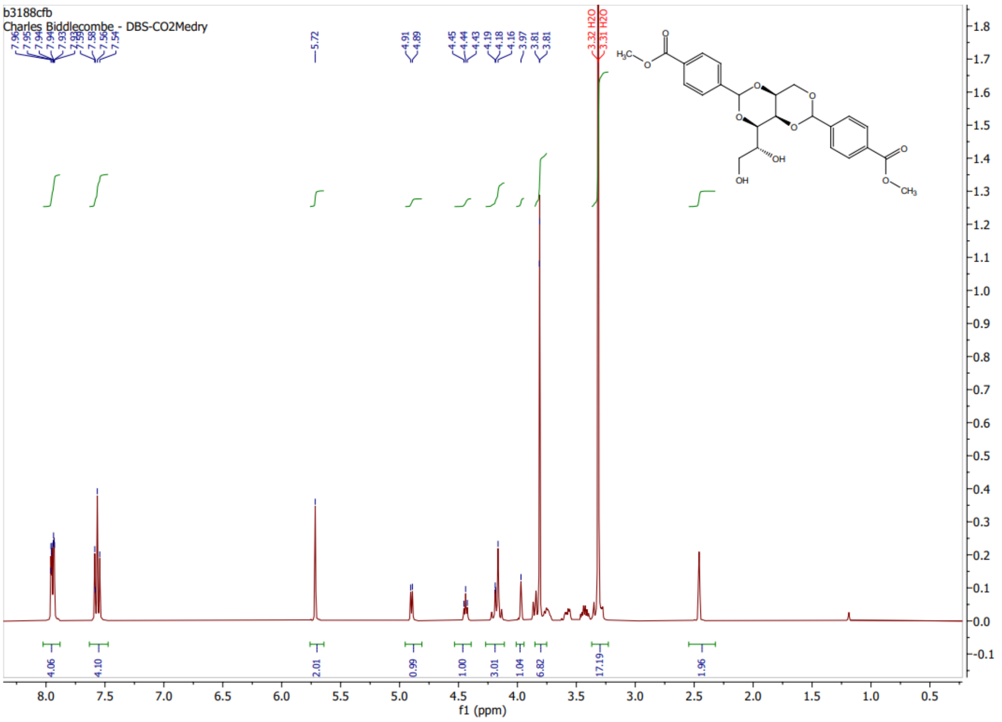

Figure 6.1 - DBS-CO$_2$Me ^{1}H NMR (400 MHz, DMSO-d$_6$)

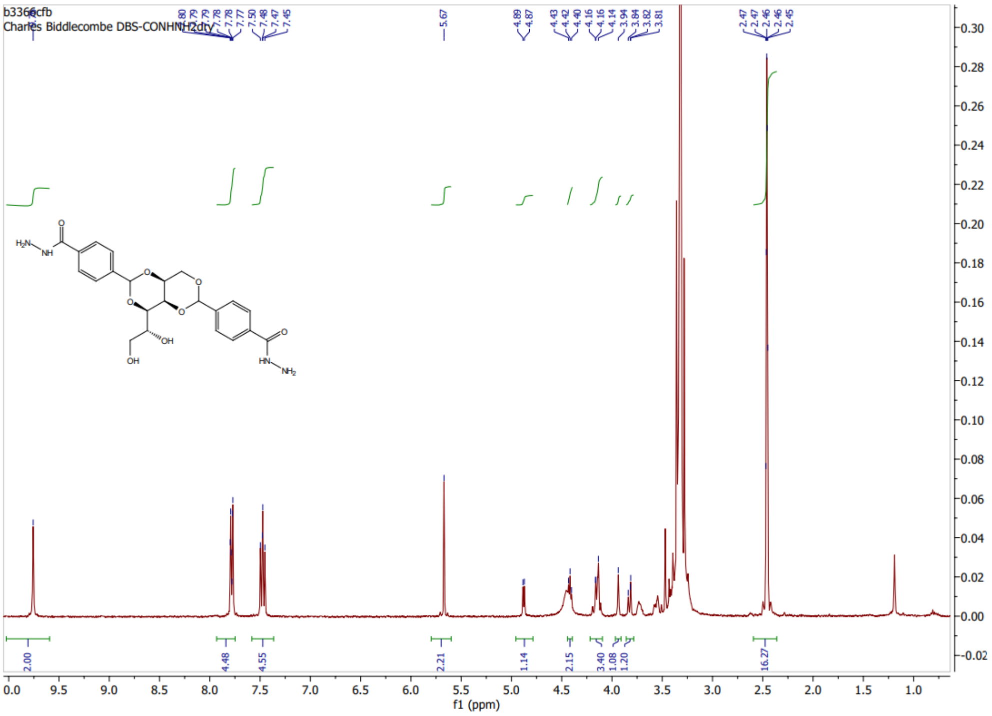

Figure 6.2 - DBS-CONHNH$_2$ ^{1}H NMR (400 MHz, DMSO-d$_6$)

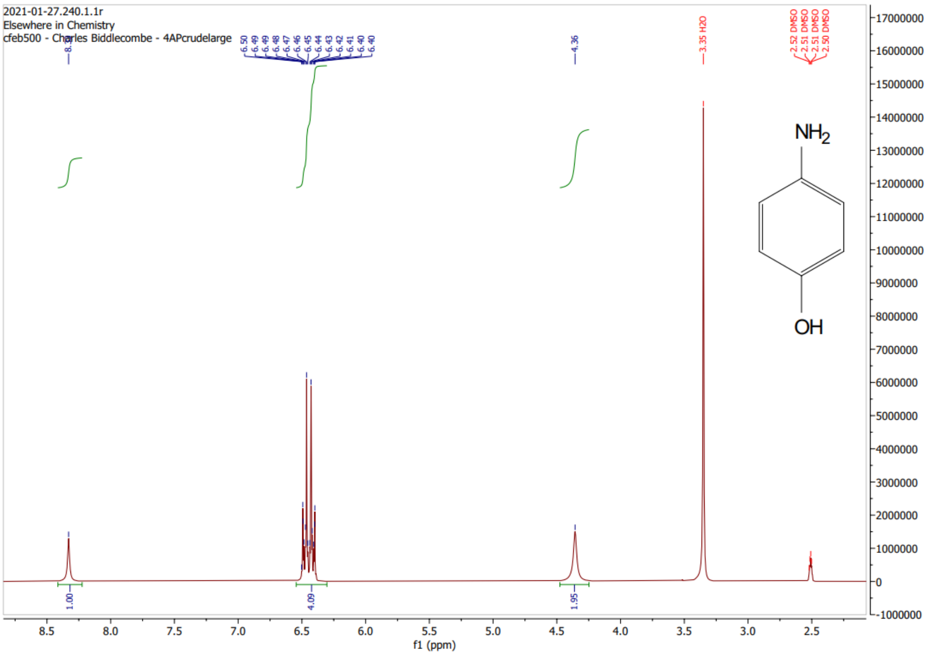

Figure 6.3 - 4-aminophenol ^{1}H NMR (400 MHz, DMSO-d_6)

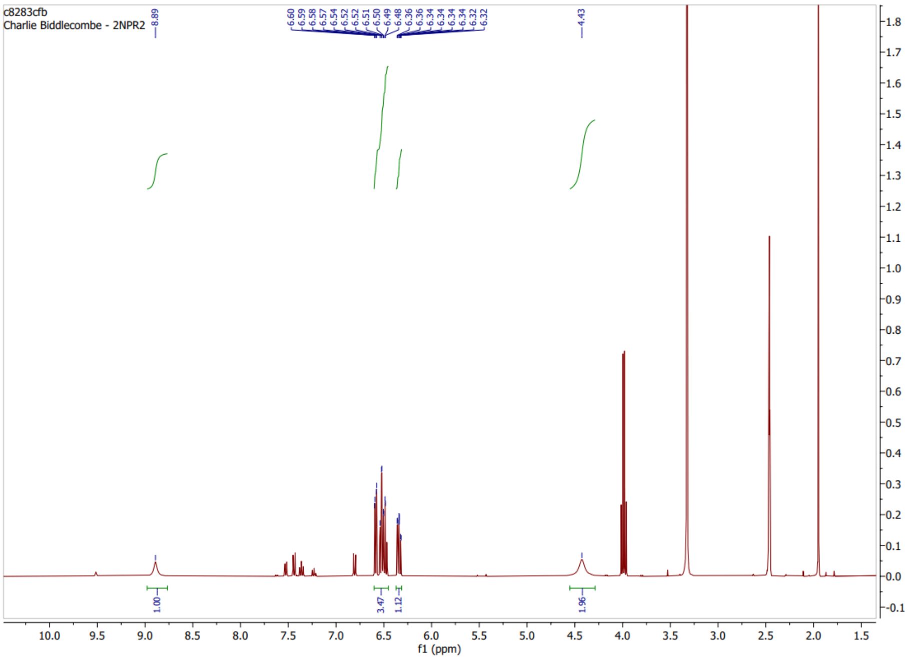

Figure 6.4 - 2-aminophenol ^{1}H NMR (400 MHz, DMSO-d_6)

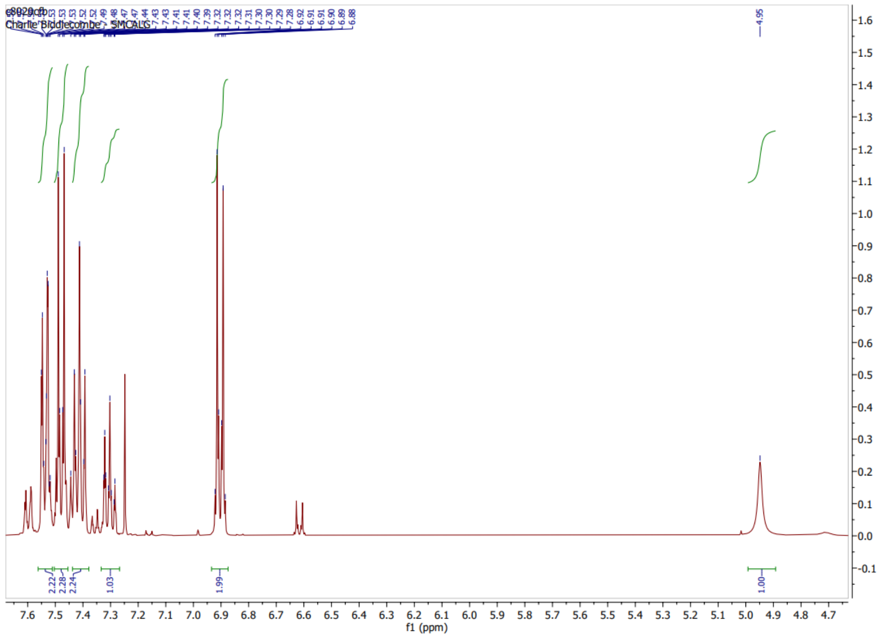

Figure 6.5 - 4-phenylphenol catalysed via Alginate Pd Beads, ^{1}H NMR (400 MHz, $CDCl_3$)

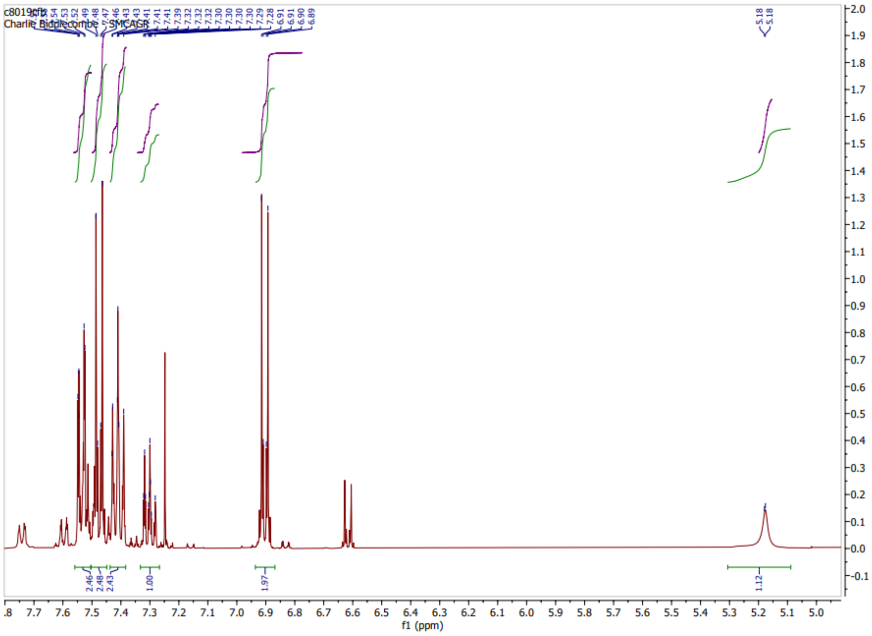

Figure 6.6 - 4-phenylphenol catalysed via Agarose Pd Beads, ^{1}H NMR (400 MHz, $CDCl_3$)

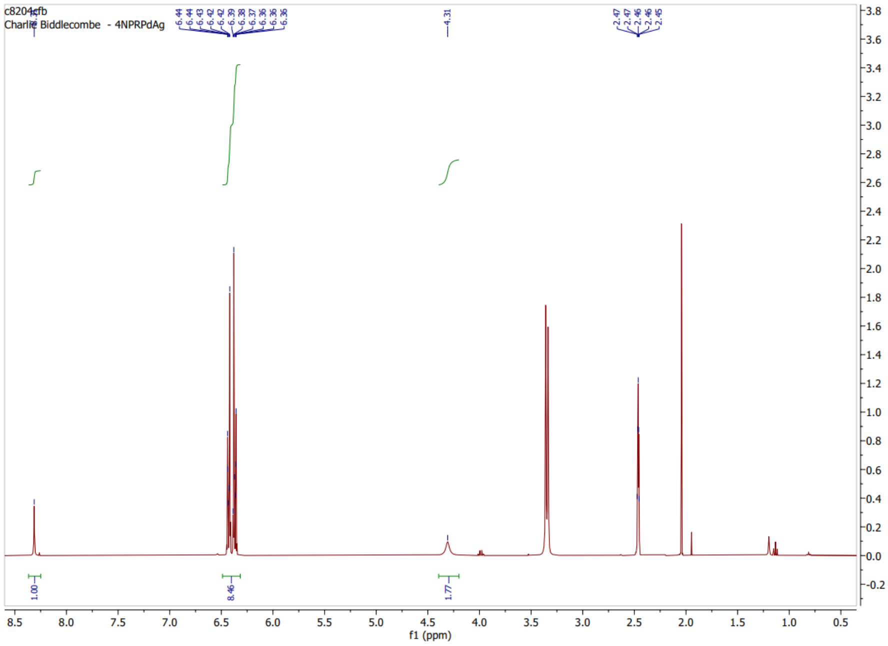

Figure 6.7 - 4-aminophenol using Ag/Pd Beads, ^{1}H NMR (400 MHz, DMSO-d_6)

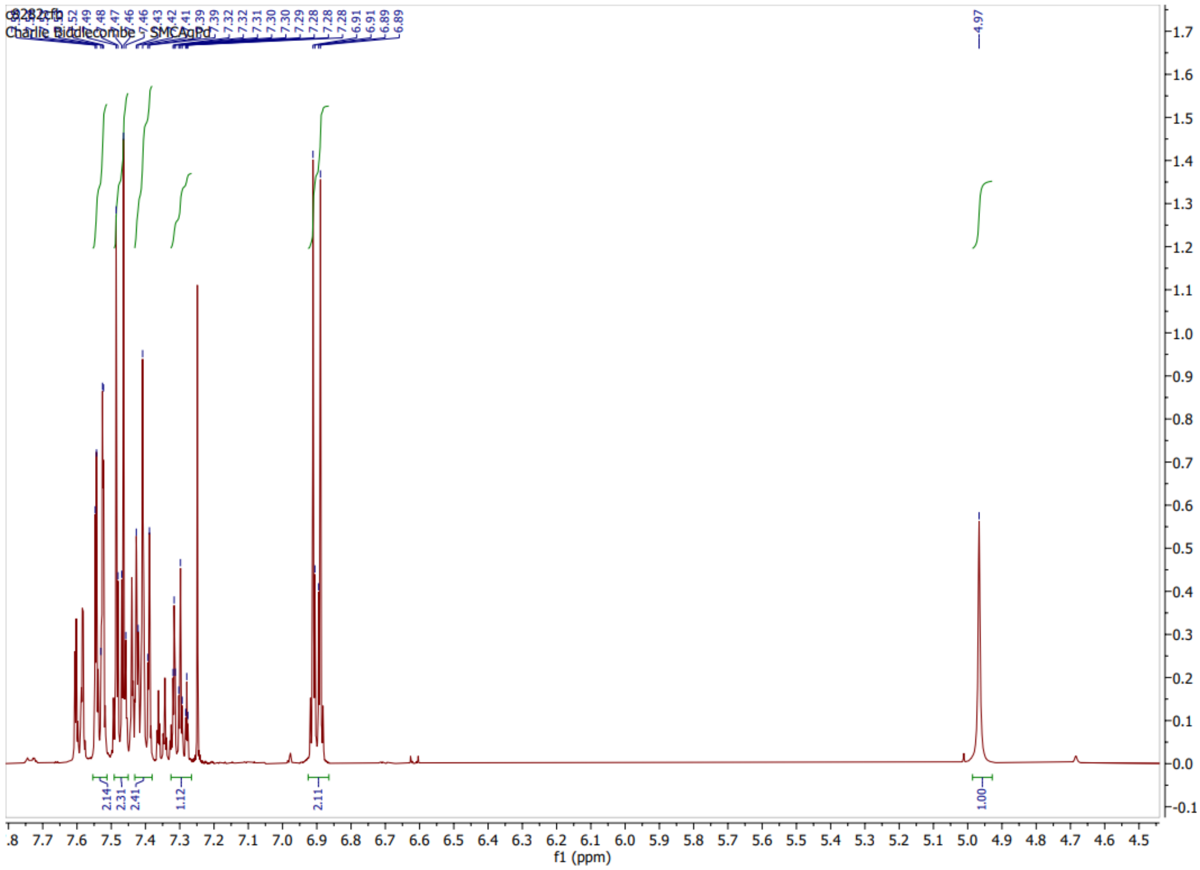

Figure 6.8 - 4-phenylphenol catalysed via Agarose Pd/Ag Beads, ^{1}H NMR (400 MHz, CDCl$_3$)

Bibliography

1 - J. Maitra, V. K. Shukla, *American Journal of Polymer Science,* 2014, 4(2), 25-31

2 - P. Gacesa, *Carbohydrate Polymers,* 1988, 8, 161-182

3 - O. Wichterle, D. Lim, *Nature*, 1960, 185, 117–118

4 - N. A. Peppas, R. E. Berner, *Biomaterials*, 1980, 1, 158-162

5 - J. Sperinde, L. G. Griffith, *Macromolecules,* 1997, 30, 5255-5264

6 - P. Caliceti, S. Salmaso, A. Lante, M. Yoshida, R. Katakai, F. Martellini, L. H. I. Mei, *J. Controlled Release*, 2001, 75, 173 –181

7 - X. Du, J. Zhou, J. Shi, B. Xu, *Chem. Rev.,* 2015, 115, 24, 13165–13307

8 - A. Dasgupta, J. H. Mondal, D. Das, *RSC Adv.*, 2013, 3, 9117-9149

9 - P. K. Gavel, D. Dev, H. S. Parmar, S. Bhasin, A. K. Das, *ACS Applied Materials & Interfaces,* 2018, *10*, 10729-10740

10 - R. Vegners, I. Shestakova, I. Kalvinsh, R. M. Ezzell, P. A. Janmey, *J. Pept. Sci.,* 1995, 1, 371–378

11 - Y. M. Abul-Haija, G.G. Scott, J. K. Sahoo, T. Tuttle, R. V. Ulijn, *Chem. Commun.*, 2017, 53, 9562-9565

12 - G.Wang, S. Cheuk, E. D. Stevens, *Carbohydrate Research*, 2009, 344, 417–425

13 - J. Morris, J. Bietsch, K. Badshaw, G. Wang, *Gels,* 2021, *7*, 24

14 - Critical Raw Materials Resilience: Charting a Path towards greater Security and Sustainability, *COM*, 2020, 474l

15 - A, B. Theberge, G. Whyte, M. Frenzel, L. M. Fidalgo, R. C. R. Wootton, W. T. S. Huck, *Chem. Commun.*, 2009, 6225-6227

16 - A. J. Sandee, D.G. I. Petra, J. N. H. Reek, P. C. J. Kamer, P. W. N. M. van Leeuwen, *Chem. Eur. J*, 2001, 7, No.6

17 - B. Escuder, F. Rodriguez-Llansola, J. F. Miravet, *New J. Chem.*, 2010,34, 1044-1054

18 - T. Tu, W. Fang, Y. Zhang, J. Wu, C. Liu, H. Zhu, *Chem.Asian J.*, 2018, 13, 712 –729

19 - C. Rest, A. Martin, V. Stepanenko, N. K. Allampally, D. Schmidt, G. Fernandez, *Chem. Commun.*, 2014, 50, 13366-13369

20 - T. Tu, W. Assenmacher, H. Peterlik, R. Weisbarth, M. Nieger, K. H. Dötz, *Angew. Chem. Int. Ed*, 2007, 46, 6368 –6371

21 - D. Wang, D. Astruc, *Chem. Soc. Rev.*, 2017, 46, 816-854

22 - N. T. K. Thanh, N. Maclean, S. Mahiddine, *Chem. Rev*., 2014, 114, 7610−7630

23 - M. Hurata, T. Kobayashi, H. Sano, N. Yamada, *Chem. Lett.*, 1987, 16, 405−408

24 - B. Chaudret, J. M. Asensio, D. Bouzouita, P. W. N. M. van Leeuwen, *Chem. Rev.* 2020, 120, 2, 1042–1084

25 - A. Balanta, C. Godard, C. Claver, *Chem. Soc. Rev.*, 2011, 40, 4973-4985

26 - B. C. Ranu, R. Dey, K. Chattopadhyay, *Tetrahedron Lett.*, 2008, 49, 3430

27 - M. R. Reithofer, A. Lakshmanan, A. T. K. Ping, J. M. Chin, C. Hauser, *Biomaterials,* 2014, 35, 7535-7542

28 - T. Simon, C. Wu, J. Liang, C. Cheng, F. Ko, *New J. Chem.*, 2016,40, 2036-2043

29 - S. C. J. Meskers. A. P. H. J. Schennig, *Angew. Chem. Int. Ed*., 2007, 46, 1825–1828

30 - J. Puigmarti-Luis, E. Taboada, L. N. Feldborg, A. P. del Pino, A. Roig, D. B. Amabilino, *Soft Matter*, 2011, 7, 2755-2761

31 - M. C. Orilall, U. Wiesner, *Chem. Soc. Rev.*, 2011, 40, 520

32 - M. Maity, U. Maitra, *J. Mater. Chem. A*, 2014, 2, 18952-18958

33 - H. Firouzabadi, N. Iranpoor, F. Kazemi, M. Gholinejad, *Journal of Molecular Catalysis A: Chemical*, 2012, 357, 154–161

34 - Q. Li, J. Ding, L. Zhao, X. Li, Q. Yue, B. Gao, *RSC Adv.*, 2017,7, 17599-17611

35 - M. J. Meunier, *Ann. Chim. Phys*., 1891, 22, 412

36 - B. O. Okesola, V. M. P. Vieira, D. J. Cornwell, N. K. Whitelaw, D. K. Smith, *Soft Matter*, 2015, 11, 4768

37 - B. O. Okesola, D. J. Cornwell, D. K. Smith, *Soft Matter*, 2013, 9, 8730

38 - B. O. Okesola, D. K. Smith, *Chem. Commun*., 2013, 49, 11164

39 - B. O. Okesola, S. K. Suravaram, A. Parkin, D. K. Smith, *Angew. Chem. Int. Ed*. 2016, 55, 183 –187

40 - A. Banerjee, S. Paul, K. Basu, K. S. Das, *ChemNanoMat*, 2018, 4, 882 – 887

41 - P. Slavik. D. W. Kurka, D. K. Smith, *Chem. Sci.*, 2018,9, 8673-8681

42 - P. Slavik, D. K. Smith, *Tetrahedron*, 2020, 76, 131344

43 - C. C. Piras, C. S. Mahon, D. K. Smith, *Chem. Eur. J*., 2020, 26, 8452 – 8457

44 - M. Ghorbanloo, A. Heydari, H. Yahiro, *Appl. Organometal. Chem*. 2018, 32, 3917

45 - D. J. Cornwell, D. K. Smith, *Mater. Horiz.*, 2015,2, 279-293

46 - C. L. Feng, P. Li, X. D, Y. Tang, S. Zhu, J. Gu, D. Zhang, *Journal of Colloid and Interface Science*, 2012, 387, 115–122

47 - B. P. Nowak, B. J. Ravoo, *Soft Matter*, 2020,16, 7299-7304

48 - V. M. P. Vieira, A. C. Lima, M. De Jong, D. K. Smith, *Chem. Eur. J.*, 2018, 24, 15112–15118

49 - C. Piras, P. Slavik, D. K. Smith, *Angew. Chem. Int. Ed*. 2020, 59, 853 – 859

50 - C. Piras, D. K. Smith, *Chem. Eur. J.,* 2021, 27, 14527–14534

51 – K. Ensumi, R. Isono, T. Yoshimura, *Langmuir,* 2004, 20, 237-243

52 – X. Kong, Z. Sun, M. Chen, C. Chen, Q. Chen, *Energy Environ. Sci.***,** 2013,6, 3260-3266

53 - D. Blakemore, *RSC*, 2016, 1, 1-69

54 - Q. Wang, C. Liao, Y. Mao, T. Su, Q. Wu, *Chem. Commun.*, 2014, 50, 14429-14432